Intercalibration Campaign for Gas Concentration Measurements in Lake Kivu Lead authors Co-authors Citation Content

Martin Schmid, Fabian Bärenbold, Bertram Boehrer, François Darchambeau, Roberto Grilli, Jack Triest, Wolf von Tümpling

Intercalibration Campaign for Gas Concentration Measurements in Lake Kivu

Lead authors

Martin Schmid, and Fabian Bärenbold

Eawag: Swiss Federal Institute of Aquatic Science and Technology, Surface Waters – Research and Management, Kastanienbaum Switzerland

Bertram Boehrer

Helmholtz-Centre for Environmental Research – UFZ, Magdeburg, Germany

Co-authors

François Darchambeau

KivuWatt Ltd., Kigali, Rwanda and Chemical Oceanography Unit, Université de Liège, Belgium

Roberto Grilli

Institut des Géosciences de l'Environnement (IGE), CNRS, Grenoble France.

Jack Triest

KM Contros, Kongsberg Maritime, Kiel, Germany

Wolf von Tümpling

Helmholtz-Centre for Environmental Research – UFZ, Magdeburg, Germany

18 January 2019

Citation

Schmid M, Bärenbold F, Boehrer B, Darchambeau F, Grilli R, Triest J, von Tümpling W (2019). Intercalibration Campaign for Gas Concentration Measurements in Lake Kivu, Report prepared for the Lake Kivu Monitoring Programme (LKMP) of the Energy Development Corporation Limited (EDCL), Kigali, Rwanda.

Content

Executive Summary

1. The 2018 intercalibration campaign aimed at quantifying the methane (CH_4) and carbon dioxide (CO_2) gas content and the recharge rate of CH_4 in Lake Kivu using a range of different measurement methods. Measurements were performed by research teams from the Helmholtz Centre for Environmental Research (UFZ) in Magdeburg (Germany), the Swiss Federal Institute for Aquatic Science and Technology (Eawag, Switzerland), the French National Centre for Scientific Research (CNRS) in Grenoble (France), and from KivuWatt Ltd (Kigali, Rwanda).
2. The following measurement methods were applied: two sensors for the in-situ observation of total dissolved gas pressure; two sensors for the in-situ observation of the partial pressure of dissolved CH_4; and two methods for quantifying the concentrations of dissolved CH_4 and CO_2 in samples retrieved from the lake either using sampling bags or a tubing system. These methods were specifically customized for the application under the special conditions in Lake Kivu. Since some of the methods quantify partial pressures of CH_4 and/or CO_2, and other methods quantify their concentrations, a procedure for converting between partial pressures and concentrations was developed and implemented.
3. The observations yielded a consistent picture of the vertical profiles of dissolved concentrations of CH_4 and CO_2 as well as the total gas pressures in Lake Kivu. The observed variability between the datasets is related to the limited accuracy of the different measurement methods.
4. The observed CH_4 concentrations were within the range of previous observations. However, in the resource zone (below 260 m depth), they were approximately 5-20 % below the concentrations measured by M. Halbwachs and J.-C. Tochon in 2003, which had previously been used as the standard for estimating the CH_4 content in the lake.
5. The CH_4 content in the resource zone (between 260 and 480 m depth) was estimated to ~40 km^3 STP (volume of gas at a temperature of 0°C and a pressure of 1 atm) (range, 36.4 - 42.2 km^3). These numbers are somewhat lower than the previous estimate of 44.7 km^3 by Wüest and Schmid (2012) based on the measurements of M. Halbwachs and J.-C. Tochon in 2003. The CH_4 content in the potential resource zone (200-260 m) was estimated to range between 8.2 and 8.6 km^3 for all methods, which agrees with the previous estimate of 8.5 km^3. The whole-lake CO_2 content was estimated to 285 km^3 STP.
6. The differences in CH_4 concentrations and content compared to previous estimates are due to the limited accuracy of the different measurement methods and were not caused by the comparably small amount of CH_4 removed by the past and ongoing gas extraction operations.
7. The 2018 measurements do not confirm the previous hypothesis that the CH_4 concentrations were increasing during the last decades in Lake Kivu. They rather indicate approximately constant concentrations since the first observations in the 1950's within the uncertainty range of the present and previous measurements.
8. Recommendations for monitoring the evolution of gas concentrations in the lake cover two important aspects. Required monitoring equipment and frequency are defined based on different monitoring purposes. In addition, a need for building up sampling routines and skills is identified.

1. Introduction

1.1. Background

Lake Kivu, situated in East Africa on the border between Rwanda and the Democratic Republic of the Congo, contains large amounts of dissolved gases, mainly carbon dioxide (CO_2) and methane (CH_4) in its permanently stratified deep water. These gases are of high relevance for two reasons. First, they pose a risk for the local population, as they could potentially erupt from the lake with catastrophic consequences. Second, the CH_4 is an important energy resource. The commercial-scale exploitation of this resource was started on 31 December 2015 with the commencement of the operation of the KivuWatt power plant Phase 1 with an installed capacity of 26 MW.

The management of the gas resource in Lake Kivu up to now is mainly based on the gas concentrations measured in November 2003 by the team of Michel Halbwachs and published by Schmid et al. (2005). Furthermore, from a comparison of these observations with those made by Klaus Tietze in 1974/5 (Tietze, 1978), Schmid et al. (2005) concluded that CH_4 concentrations seemed to have increased by up to 15 % within three decades, potentially leading to an increased risk of a gas eruption. Based on a more detailed analysis of the carbon budget of the lake, Pasche et al. (2011) subsequently concluded that the concentrations are likely not increasing as fast as previously suspected.

Gas extraction from Lake Kivu is expected to be further developed in the near future. The second phase of the KivuWatt project may reach a total capacity of 100 MW. Another concession agreement has been signed between the Government of Rwanda and Symbion for a capacity of 56 MW. Further concessions are being negotiated by the Governments of both Rwanda and the Democratic Republic of the Congo. Given this current interest to further develop CH_4 extraction from the lake, it is important to re-assess the gas concentrations in the lake and to agree on accurate methods for monitoring their evolution.

With this aim, the Lake Kivu Monitoring Programme (LKMP) of the Energy Development Corporation Limited (EDCL), a subsidiary of the Rwanda Energy Group (REG), has initiated the present intercalibration campaign. The aims of this campaign are the following:

- Measure the concentrations of dissolved CH_4 and CO_2 in Lake Kivu using different state-of-the-art methods
- Derive a best estimate and an uncertainty range for the concentrations of dissolved CH_4 and CO_2, and the total amount of dissolved gases in the lake
- Derive a best estimate for the evolution of dissolved CH_4 in the lake based on the current and previous measurements
- Assess the advantages and disadvantages of the different methods and discuss their possible use for monitoring the gas concentrations in the lake in the future

1.2. Previous gas measurements

Gas concentrations in Lake Kivu were previously measured and published by several different research teams. An overview of the available measurements is given in Table 1.1.

Table 1.1: Overview of previously published measurements of gas concentrations in Lake Kivu.

Years	Institution	Measured gases	Publications	Comments
1935	Université de Liège	CO_2	Damas (1937)	Samples degassed before measurement: strong underestimation of concentrations.
1952-4	Institut royal des Sciences naturelles de Belgique	CH_4, CO_2	Schmitz and Kufferath (1955)	Only includes the gases that exsolved under local atmospheric pressure (small error for CH_4, larger error for CO_2).
1971	Woods Hole Oceanographic Institute (WHOI)	CH_4, CO_2, N_2, H_2S, alkanes	Degens et al. (1971); Degens et al. (1973)	CH_4 concentrations listed in Table 2 of Degens et al. (1971) disagree with those plotted in Figure 6 of Degens et al. (1973)
1974/5	Bundesanstalt für Geowissenschaften und Rohstoffe	CH_4, CO_2, N_2, alkanes	Tietze (1978); Tietze et al. (1980)	Variability of the individual samples in the deep water exceeds the estimated accuracy of 5 %
1990	USGS	CH_4, CO_2, N_2, He, H_2, Ar, C_2H_6, C_3H_8, H_2S	Tuttle et al. (1990)	Only a few individual samples
2003	Université de Savoie - M. Halbwachs and J.-C. Tochon	CH_4, CO_2	Schmid et al. (2005)	No detailed method description published.
2004	Eawag	CH_4, CO_2	Schmid et al. (2005)	CH_4 measurements with in-situ sensor with slow relaxation time (46 minutes) CO_2 calculated from pH and alkalinity.
2006	Eawag	CH_4	Pasche et al. (2011)	Samples were degassing before measurement, concentrations in the deeper layers are therefore underestimated.
2004-7	University of Florence (and others)	CH_4, CO_2, Ar, O_2, N_2, He, Ne, alkanes	Tassi et al. (2009)	Measurements made in different basins of the lake; results seem to indicate contamination with air.

Three general principles have been applied for measuring gas concentrations in Lake Kivu:

1) Taking water samples in-situ under pressure, bringing them to the surface and quantitatively measure the gas amounts contained in the water samples. Variants of this method were applied by Schmitz and Kufferath (1955), Degens et al. (1971), and Tietze (1978). The measurements by Klaus Tietze are certainly those where the largest effort was made to reduce the measurement uncertainty. Water samples were degassed and the gas volumes measured with an apparatus that was specifically designed for this purpose. Gas concentrations were determined with gas chromatography. Tietze (1978) estimated the standard deviation of the gas measurements to 5 %.

2) Transferring water samples through tubes to the lake surface, where they are degassed under atmospheric pressure. Concentrations in the gas phase as well as the flows of water and gas are measured, the remaining concentrations in the water phase are either measured as well or assumed to be in equilibrium with the gas phase. Variants of this method were applied by M. Halbwachs and J.-C. Tochon (results published in Schmid et al., 2005) and by Tassi et al. (2009). The measurements by Halbwachs and Tochon showed a very high reproducibility. Their uncertainty was estimated to be ± 4 % (Schmid et al., 2005).

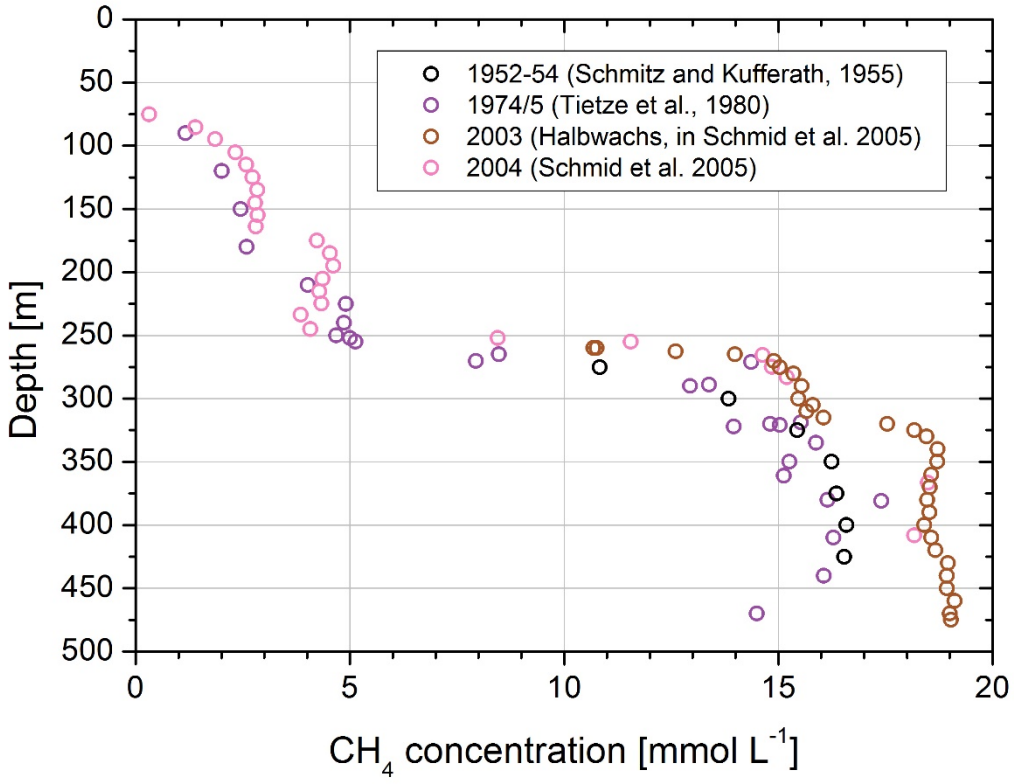

Figure 1.1: Selected previous observations of CH_4 concentrations in Lake Kivu. The measurements of K. Tietze were digitized from Tietze et al. (1980), since the numeric values were not available.

3) Measuring gas concentrations with in-situ sensors (e.g. Schmid et al., 2005). These sensors generally contain a measurement volume separated from the water by a gas-permeable membrane. Gas pressures or mixing ratios within this volume are then determined with various methods. The calibration of these sensors for measurements in Lake Kivu is a challenge, since conditions in the deep-water of the lake with pressures up to 50 bar and high gas concentrations are not easily reproducible in the laboratory. Also, often long sampling times are required for equilibrating the gas volume in the sensors with the water, or else the concentrations have to be extrapolated from the observed exponential approach towards the equilibrium concentration, as was done by Schmid et al. (2005).

CO_2 concentrations can also be estimated by measuring alkalinity and pH. If alkalinity is mainly determined by the carbonate system, as it is the case in Lake Kivu, the concentrations of all carbonate species can be calculated from their chemical equilibria if pH and alkalinity are known. The problem with this approach for the case of Lake Kivu is that the pH in the deep water is close to the first dissociation constant for the deprotonation of aqueous CO_2 (H_2CO_3). This results in a large uncertainty of the calculated CO_2 concentration already for small uncertainties in the measured pH (Figure 1.2).

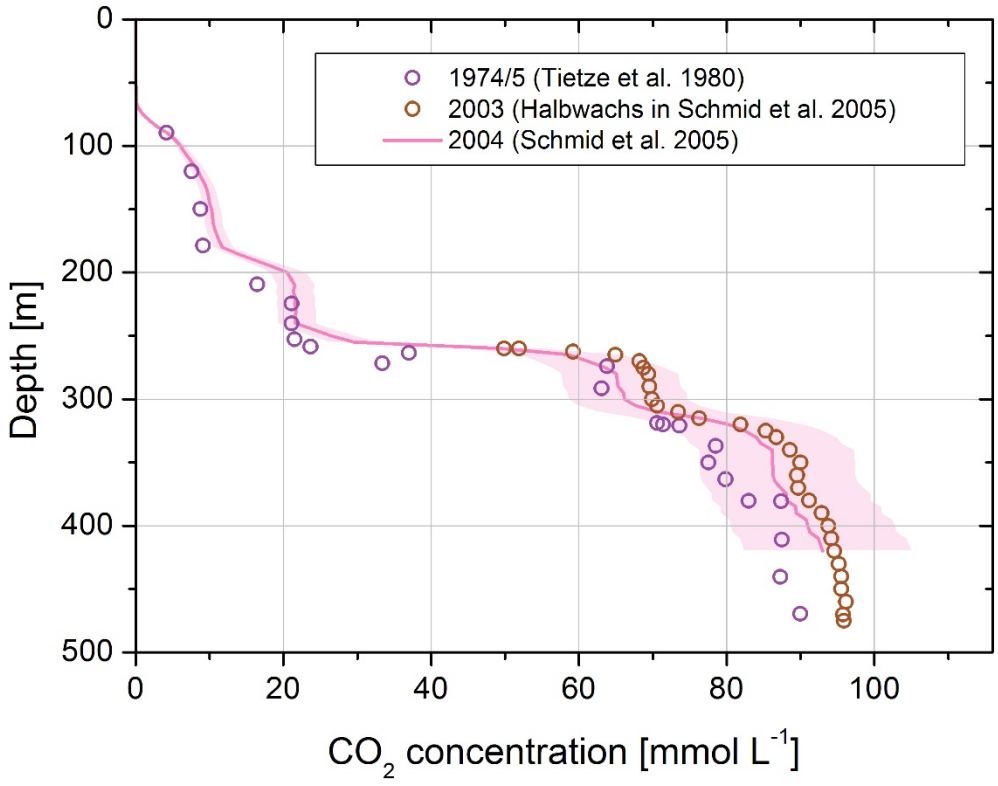

Figure 1.2: Selected previous observations of CO_2 concentrations in Lake Kivu. The measurements of K. Tietze were digitized from Tietze et al. (1980), since the numeric values were not available. The grey area shows the variation of the CO_2 concentrations calculated from alkalinity and pH measurements if the pH is varied by ± 0.05, indicating the strong dependence of this estimate on the precision of the pH measurement.

2. Methods

2.1. Sampling Site and Procedure

The measurement campaign took place from 9 to 13 March 2018 (Eawag conducted measurements until 18 March) and from 8 to 11 May 2018 (only KivuWatt's team) near Gisenyi/Rubavu at the Northern shore of Lake Kivu in Rwanda. All participating institutions and researchers are listed in Table 2.1.

Table 2.1: Participants at measurement campaign in March 2018

Institution	**Participants**
UFZ Magdeburg	Dr. Bertram Boehrer, Dr. Wolf von Tümpling
CNRS Grenoble	Dr. Roberto Grilli
KivuWatt	Dr. François Darchambeau, Placid Nkusi
Eawag	Fabian Bärenbold, Reto Britt, Michael Plüss

The goal of the campaign was to obtain at least one vertical profile of gas concentrations for each method for the purpose of inter-comparison between the different methods. The gas profiles should be measured at a location representative for the entire lake and cover as much as possible of the full depth of 485 m. Thus, the measurement site needed to be deep, distant from any known subaquatic source but still well accessible by boat. It turned out that the combination of the two measurement sites listed in Table 2.2 best fulfilled the criteria mentioned above: site 1 is equipped with a research platform and is well accessible, while site 2 is further away and deeper. All teams worked at site 1, but UFZ, KivuWatt and Eawag also went to site 2 to sample down to 450 m depth.

Table 2.2: Measurement sites

	Depth [m]	**Working on:**	**Distance from Gisenyi**	**Coordinates**
Site 1	410	Platform/boat	5 km	1.74087°S / 29.22602°E
Site 2	460	Boat	ca. 12 km	1.79865°S / 29.17172°E

It was agreed that the different groups would sample/measure with a vertical spacing of 20 m, starting at 10 or 70 m below the surface or at 170 m for the groups, which only sampled the deep water. However, due to problems with rope labeling and boat drift, some of the sampled depths deviated from the planned depths (up to some meters). Table 2.3 summarizes where and in which depth ranges the different groups sampled/measured.

The horizontal distance between the sites and the different sampling dates are not expected to influence comparability, as horizontal transport is much faster than vertical transport and gas production or consumption. Therefore, it is reasonable to assume horizontal and temporal steady-state for the duration of the campaign.

Table 2.3: Sampling depths and locations

Institution	Depth range	Site	Working on
UFZ	170 – 430 m	Site 1 / Site 2	Boat
CNRS	10 – 170 m	Site 1	Boat
KivuWatt	70 – 417.5 m	Site 1 / Site 2	Boat
Eawag	10 – 450 m	Site 1 / Site 2	Platform / boat

A vertical profile of temperature, electrical conductivity, oxygen concentration, pH and turbidity was measured by UFZ at Site 2 on 13 March using a multiparameter probe CTM1143 (Sea and Sun Technology, Germany; Figure 2.1). Here and in all following methods, pressure (bar) was converted to depth (m) by dividing by 0.0978 bar m^{-1}. The profile showed typical conditions for the wet season, where the surface layer of the lake (i.e., the top 60 m which can undergo seasonal mixing during the dry season) is thermally stratified (Figure 2.2). There was a steep oxycline with strongly decreasing oxygen concentrations between 25 and 40 m depth, and below about 45 m depth, the water column was anoxic. Below 60 m depth, the profile showed the usual stepwise increase in temperature and conductivity and decrease in pH.

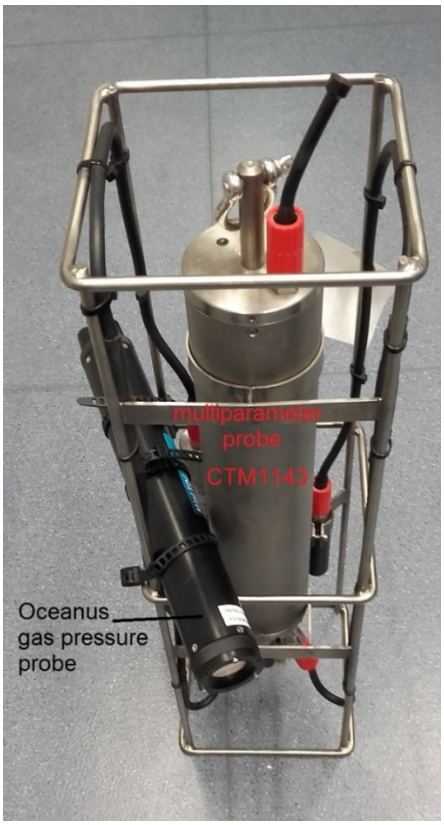

Figure 2.1: Multiparameter probe CTM1143 (Sea and Sun Technology, Germany) used for profiles of depth (pressure), temperature, electrical conductivity, oxygen concentration, pH and other parameters in Lake Kivu, with Pro-Oceanus total dissolved gas pressure (Mini-TDGP) sensor attached.

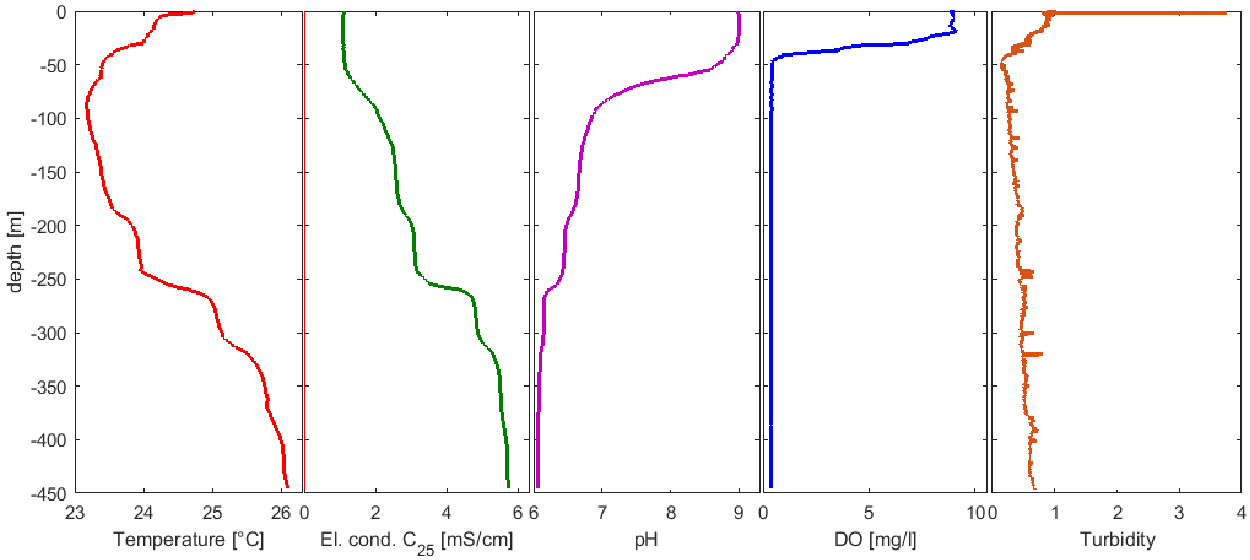

Figure 2.2: Profiles of in-situ temperature, electrical conductivity (temperature compensated for 25°C), pH, dissolved oxygen concentration and turbidity of Lake Kivu water against depth. The profiles were measured with a multiparameter probe (CTM1143, Sea and Sun Technology, Germany) on 13th March 2018 close to Site 2.

2.2. In-situ gas pressure

In-situ gas pressure measurements were performed by UFZ Magdeburg using a Pro-Oceanus sensor, and by KivuWatt using a Contros sensor.

Pro-Oceanus customized their gas pressure sensor for the application in Lake Kivu, as standard sensors for total dissolved gas pressure (TDGP) are usually not designed for the deployment depths and expected gas pressures in Lake Kivu. The pressure sensor contains a gas volume separated from the lake water by a membrane, which is easily permeable for dissolved gases such as CH_4, CO_2 and N_2. The partial pressures of all gases in the measurement volume adjust such that their fugacity in the gas space is in equilibrium with their concentrations in the water. If the total gas pressure inside the gas space equalled the outside pressure (hydrostatic plus atmospheric pressure), a virtual gas bubble would withstand the pressure at depth and start moving upwards through the water column. Hence, the ratio of the total pressure inside the measurement volume compared to absolute pressure represents a quantification of the distance of lake water to spontaneous ebullition.

Before deployment, the sensor needed to be immersed in water for several hours. Thereafter, a response time of only few minutes was expected. Measurements were performed from the platform (site 1) at

discrete depths where the probe was left for about 20 to 30 min (Figure 2.3). Data were recorded continuously, and from the time series at 286.1 m depth, a response time of less than 4 min (half-value time $t_{1/2}$ of 150 s) was determined by fitting an exponential curve to the observations. As the available time for measurements was limited and also the recovery of the sensor required time, measurements were done at seven discrete depths. The CTM1143 probe accompanied the TDGP sensor for an accurate depth reference (Figure 2.1).

In order to compensate for the measured response time, the total gas pressure TDGP at time t was calculated from the measured pressures p_{meas} at the times t and t - $t_{1/2}$ using equation (1).

$$\mathrm{TDGP}\ (\mathrm{t}) = 2\, p_{meas}(t) - p_{meas}\left(t - t_{1/2}\right) \qquad (1)$$

As shown in Figure 2.3, TDGP (olive line) approaches the final value much faster than the original readings p_{meas} (black line).

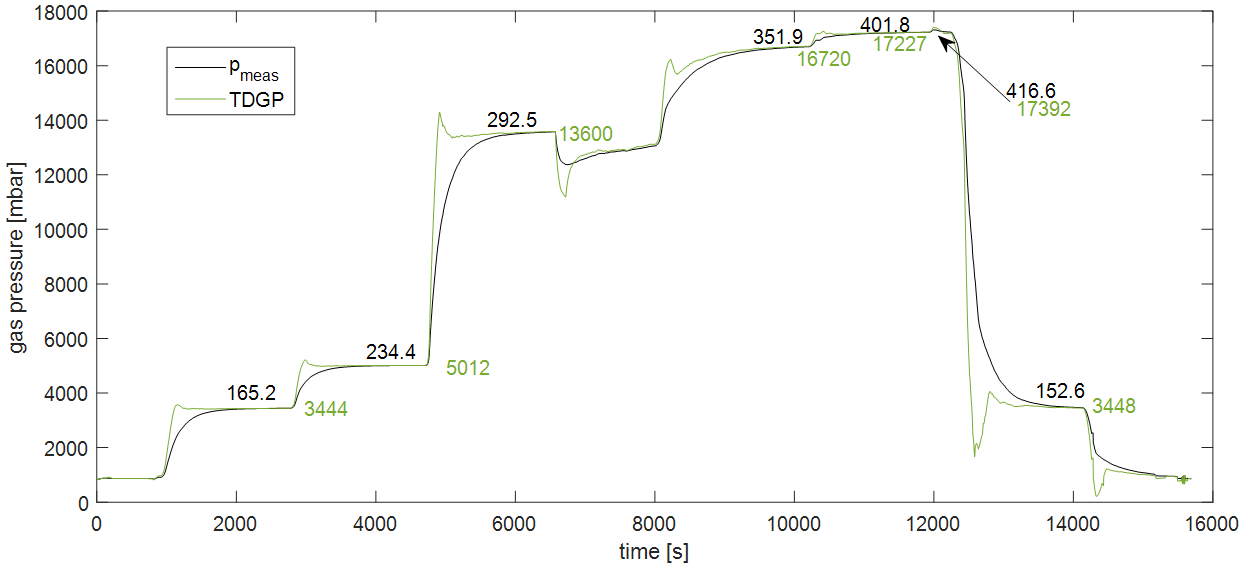

Figure 2.3: Continuously acquired gas pressure data (p_{meas}) from the custom made Pro-Oceanus TDGP probe (black line); TDGP data compensated for response time (olive coloured line); depths (m) from CTD measurements (black numbers); extrapolated total dissolved gas pressures (mbar) at the corresponding depths (olive numbers).

In-situ total gas pressures were also measured as an additional product of the Contros HydroC™-CH_4 HP sensor used by KivuWatt (section 2.3).

2.3. In-situ partial pressures of methane using a Contros in-situ sensor

These measurements were performed by the team from KivuWatt.

The CH_4 partial pressure was in-situ estimated using a Contros HydroC™-CH_4 HP system. The HydroC™ HP system is an optical, headspace-based underwater sensor for the measurement of high partial pressures of gas. Dissolved gas diffuses from the liquid through a proprietary thin film composite membrane into an internal gas cell. Therein the total dissolved gas pressure and the partial pressure of CH_4 gas are measured by a pressure sensor and a non-dispersive infrared spectrometer, respectively.

The CH_4 sensor is similar to the HydroC-CO_2 sensor presented in Fietzek et al. (2014), except for the absence of an internal zeroing system and a CH_4-specific fixed narrow-band spectral filter from 3.3-3.4 µm. The sensor range is 0-100 %. The sensor was calibrated in October 2012 and November 2015 by the manufacturer (Figure 2.4). The calibrations were made using a specially designed pressure chamber with fresh water brought to pressure using compressed target gas. Three standard gas mixtures of CO_2, CH_4 and N_2 (100 % pressure N_2; 50 % pressure CH_4 and 50 % pressure CO_2; 100 % pressure CH_4) were used to equilibrate the water volume along a gas pressure gradient (5-6 points) from 1 up to 30 bars and partial pressures of CH_4 from 0.5 to 18 bars. A polynomial function was fitted with the total gas pressure (2^{nd} order) and CH_4 signal (4^{th} order) as the independent factorial variables and the CH_4 partial pressure as the dependent variable (Figure 2.4). Because the true function between 50 % and 100 % CH_4 pressure standards is not known, a systematic error could result which probably does not exceed 10 %. The calibration results showed the absence of a significant drift of the sensor (< 3 % within the Lake Kivu gas concentration range) between the October 2012 and November 2015 calibrations. Also, KivuWatt carried out several CH_4 profiles in Lake Kivu from 2016 to 2018 using the HydroC CH_4-sensor and the repeatability of the observed CH_4 partial pressures were remarkable (standard deviation 1.9 % below the main density gradient; KivuWatt pers. comm.).

The HydroC-CH_4 system was mounted on a SeaBird 19plus V2 SeaCAT CTD profiler equipped with a SBE 43 Dissolved Oxygen sensor and a SBE 18 pH sensor. Calibrations of the SeaBird sensors were performed following manufacturer instructions. Water circulation in front of the HydroC membrane was provided by a SeaBird 5T pump, ensuring a homogeneous water flow to the membrane. A zero calibration of the HydroC-CH_4 system was made daily before each deployment using surface waters. The sampling rate was 1 Hz. The steady-state of the sensor was generally reached within 40 minutes and real-time data communication using an electromechanical cable allowed us to adjust the waiting time at each depth accordingly. In all cases, the waiting time for each depth never exceeded 1 hour. The retained partial pressure of CH_4 is the average for the last 5 min of the equilibration curve.

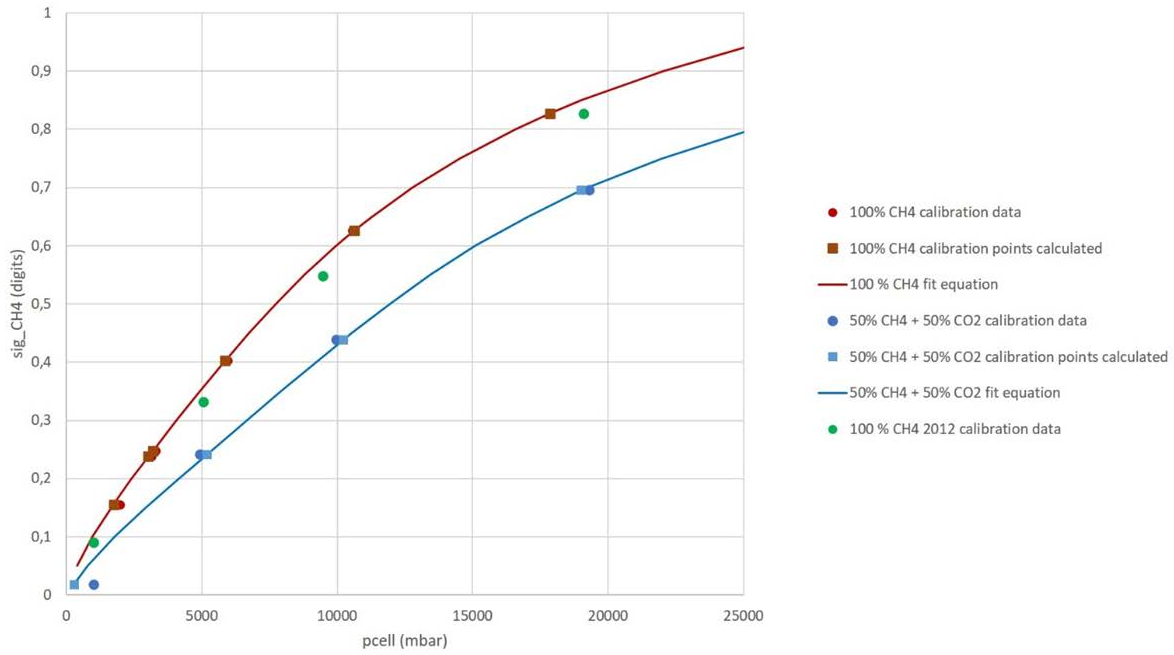

Figure 2.4: November 2015 calibration curves of the KivuWatt Contros HydroC-CH_4 sensor from 1 to 25 bars total gas pressure for the 100 % pressure CH_4 (red points) and 50 % pressure CH_4 / 50 % pressure CO_2 (blue points) gas calibration mixtures. Green points are calibration points from 2012. The observed CH_4 signal was correlated with the total and CH_4 gas pressure ($R^2 > 0.99$).

2.4. In-situ methane concentrations using a Sub-Ocean prototype sensor

2.4.1. Introduction

These measurements were performed by the team from CNRS.

It should be noted that laboratory calibration on dissolved gas measurement were performed at low concentration (full calibration up to 0.1 % of CH_4). The optical spectrometer was then re-tuned for allowing concentrations compatible with those found at Lake Kivu and calibrated with high concentrated standards (5 % of CH_4 in Ar and further diluted in zero air in the laboratory and 40 % of CH_4 in CO_2 at the LKMP Laboratory). More details about the instrument, calibrations and validation against standard techniques can be found in Grilli et al. (2018).

2.4.2. In-situ sensor

A schematic of the in situ sensor is reported in Figure 2.5. The optical instrument used in this study is based on the OFCEAS technique (optical feedback cavity enhanced absorption spectroscopy; Grilli et al., 2014) made for trace gas sensing. The dissolved air from the extraction unit (discussed below) was continuously pumped to the optical cavity of the spectrometer. The internal volume of the cell is less than 20 cm^3 and provides sample residence times < 30 sec for optimal running conditions (combination of pressure and total gas flow).

Extraction of dissolved gases from water is performed using a silicon rubber membrane. The extraction technique does not rely on gas equilibration across the membrane but, in order to achieve fast response, the dry side of the membrane is maintained at low pressure while continuously flushing it with dry 'zero' air (Triest et al. 2017). The pressure at the membrane dry side controls the total flow of dry and wet air through the membrane, and the system is designed to keep this pressure constant. While the spectrometer operates at about 20 mbar, the pressure against the dry side of the membrane is maintained at about 30 mbar.

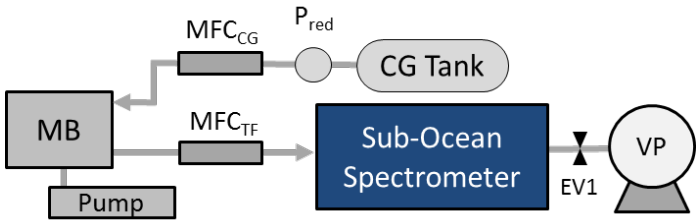

Figure 2.5: A schematic of the Sub-Ocean Sensor. MB is the membrane block where the gas extraction occurs. Water is circulating using a pump. The carrier gas (CG) flow is controlled by a mass flow controller (MFC_{CG}) and the MFC_{TF} is used for controlling the total gas flow. The low pressure on the optical spectrometer is provided by a vacuum pump (VP) and an electronic valve (EV). P_{red} is a pressure reducer.

2.4.3. Laboratory apparatus used for calibration

The schematic of the laboratory experimental setup is represented in Figure 2.6. The setup has been fully described in Grilli et al. (2018) and it is composed of a 14 L aluminium chamber, where the extraction part of the sensor (constituted by the membrane block (MB) and the water pump) is immersed in 8 L of water under controlled conditions (of pressure, temperature and salinity). The water is continuously bubbled with a gas mixture composed of zero air (N_2 + O_2, ALPHAGAZ 2, Air Liquide) and synthetic air containing CH_4 at concentrations between 0 and 0.1 % (AirLiquide) by means of a diffuser installed at the bottom of the chamber. The diffuser reduces the bubble size and therefore the time required for saturating the water with the bubbled gas mixture. The dilution system consists of two mass-flow-controllers (MFC1 and MFC2, Bronkhorst) delivering up to 100 cm^3 STP/min of gas. Water circulation was provided by the SBE 5T pump, ensuring homogeneous concentrations in the chamber. The pump and the diffuser were positioned at maximum distance from each other to allow the best homogeneity of the water sample during the measurement, and to avoid trapping air bubbles in the extraction system. The water circulated on the wet sides of the membranes (included in the membrane block), while dissolved gases were extracted on the dry side and further transferred to the Sub-Ocean spectrometer. A dry carrier gas flow (zero air, ALPHAGAZ 2, Air Liquide) was supplied by a 0-10 cm^3 STP/min mass flow controller (MFC_{CG}) to the dry side of the membrane extraction system, for continuously flushing the permeated gases from the membrane. This maintained CH_4 partial gas pressures at the lowest possible level on the dry side of the membrane in order to optimize the extraction efficiency and response time. A flowmeter (IQF+, Bronkhorst) was used for monitoring the total gas flow (composed by the carrier gas plus the dry and wet components of the extracted mixture, MFC_{TF}). CH_4 concentration in the headspace of the calibration chamber was

continuously monitored by a laser spectrometer based on the same principle as the Sub-Ocean instrument, but designed for laboratory purposes (headspace spectrometer in Figure 2.6). 10 cm^3 STP/min of the headspace gas was supplied to the headspace spectrometer, while the overflow was sent to an exhaust vent.

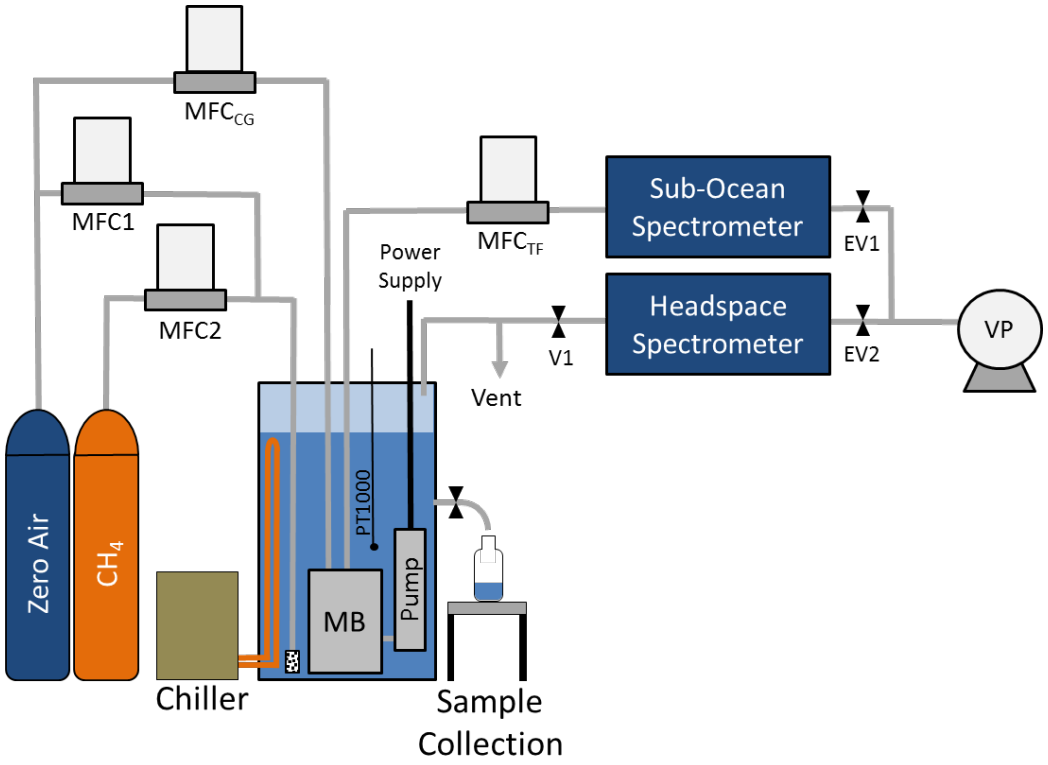

Figure 2.6: Experimental setup for laboratory tests. Two mass flow controllers (MFC1 and MFC2) were employed to bubble different mixtures of CH_4 in air into the water sample via a diffuser placed in the liquid solution. The membrane block (MB) and the water pump are immersed into the water sample, stabilized in temperature using an external chiller unit. The dry side of the membrane is continuously flushed with a small (1 to 6 cm^3 STP/min) dry gas flow supplied by the MFC_{CG}, and the mixture (carrier gas plus extracted gas) is sent to the Sub-Ocean spectrometer. The total flow is measured by a fourth mass flow controller MFC_{TF}. A portion of the headspace CH_4 concentration is monitored using a second optical spectrometer based on the same absorption spectroscopy technique (OFCEAS), while the overflow is sent to a vent. The exhausts of the analyzers are connected to two electronic valves (EV1 and EV2) and to a vacuum pump (VP) to ensure pressure regulation in the measurements gas cells.

2.4.4. Calibration in the laboratory (for low concentrations)

Prior to the experiment, both spectrometers used in the calibration apparatus (for measuring the headspace air and the dissolved gases (Figure 2.6) were calibrated using certified standard gas (Restek, Scott/Air Liquide 99 ppmv CH_4 ± 5 %). Different concentrations were obtained with a dilution system composed by MFC1 and MFC2 (Figure 2.6) used in the calibration setup. While both spectrometers were

directly connected to the dilution system, a linear response over the whole range of concentrations was obtained with a good agreement between the two devices (slope 1.090 ± 0.0027, R^2 = 0.99995 in 2015 and slope 0.9926 ± 0.003, R^2 = 0.99989 in 2018). After each change in concentration, once equilibration of the system was achieved (2-3 hours was required depending on the flow of the bubbling mixture), CH_4 concentrations were averaged for about 10 minutes.

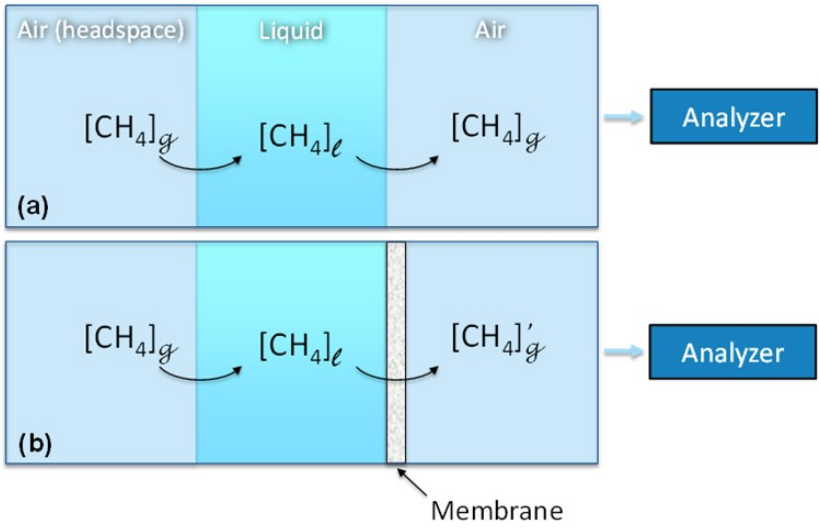

Figure 2.7: Schematic diagram showing the effect of a membrane for extracting dissolved gas. (a) represents the (ideal) case without a membrane; here, the concentration of CH_4 at equilibrium found in the analyzed gas mixture will correspond to its concentration in the headspace. (b) In the presence of a membrane, the measured CH_4 concentration will be affected by gas permeation through the membrane, resulting in a different measured concentration $[CH_4]'g$.

In order to relate the concentration of dissolved gas with respect to its abundance in the headspace in equilibrium with the liquid phase, the gas solubility in water is required. However, if we assume a system with two independent headspace volumes in contact with the same liquid volume, they will reach the same headspace concentration ($[CH_4]_g$), providing that the pressure and the temperature in the headspaces are equal. Therefore, for this experiment, knowledge of the gas solubility is not required (Figure 2.7a). The ratio $[CH_4]_g/[CH_4]_l$ ($[CH_4]_l$ being the quantity of CH_4 dissolved in water and $[CH_4]_g$ in the headspace) will depend on the solubility of CH_4 and other air components (mainly N_2, O_2, CO_2 and Ar) in water, which depends on temperature, pressure and salinity. When a membrane is positioned between the water volume and the second air reservoir (containing the air analyzed by the Sub-Ocean spectrometer; Figure 2.7b), the concentration in the latter will be affected by the membrane gas permeability. Here, the concentration of CH_4 in the gas side of the membrane will differ from that in the headspace ($[CH_4]'_g \neq [CH_4]_g$). The concentration in the dry gas downstream from the membrane can be calculated directly from the headspace concentration by using the membrane permeability coefficients for CH_4, N_2, O_2 and CO_2 (reported by Robb, 1968) and the concentration of the species in air, with the following equation:

$$[CH_4]'_g = \frac{Pr_{CH_4} \cdot [CH_4]_g}{\sum Pr_X \cdot [X]_g} \quad (2)$$

Where *Pr* values are the permeability coefficients expressed as the product of the diffusion rate times solubility and reported by Robb for 25°C and atmospheric pressure (Robb, 1968) and X are the most abundant species composing the dissolved gas mixture (N_2, O_2, Ar, CO_2). The inverse of the quantity $\frac{Pr_{CH_4}}{\sum Pr_X \cdot [X]_g}$ corresponds to the enrichment factor (m_{eff}) in equation (3), which is measured using our calibration setup for different temperatures and salinities. Concentrations, [CH_4], [X] are expressed as mixing ratios.

Measuring the concentration of water vapor $[H_2O]_g$ is required in order to retrieve the dissolved CH_4 concentration, $[CH_4]_{dissolved}$, since water vapor flow will cause dilution of the measured gas mixture (as the carrier gas flow). This measurement is performed by the same OFCEAS spectrometer embedded in the Sub-Ocean probe simultaneously to the CH_4 measurement. $[CH_4]'_{dissolved}$ is then calculated from the following equation:

$$[CH_4]'_{dissolved} = \frac{[CH_4]_{meas} \times f_t}{f_t - f_{CG} - (f_t \times [H_2O]_g)} \times \frac{1}{m_{eff}} \quad (3)$$

where $[CH_4]_{meas}$ is the methane concentration in mixing ratio measured by the optical spectrometer, f_t and f_{CG} are the total- and carrier-gas flow (ml/min) respectively, and $[H_2O]_g$ corresponds to the amount of water in mixing ratio permeating through the membrane. The complete denominator term ($f_t - f_{CG} - (f_t \times [H_2O]_g)$) corresponds to the dry flow permeating the membrane. m_{eff} represents the enrichment factor due to the membrane, and its dependency with temperature and salinity is calculated by running calibrations at different conditions (Grilli et al., 2018). From our calibration, a m_{eff} *of* 2.84 ± 0.11 for fresh water at 25°C and 1.2 bar was calculated. This is in agreement with an expected literature value of 2.76 calculated from the permeation coefficients reported by Robb (1968).

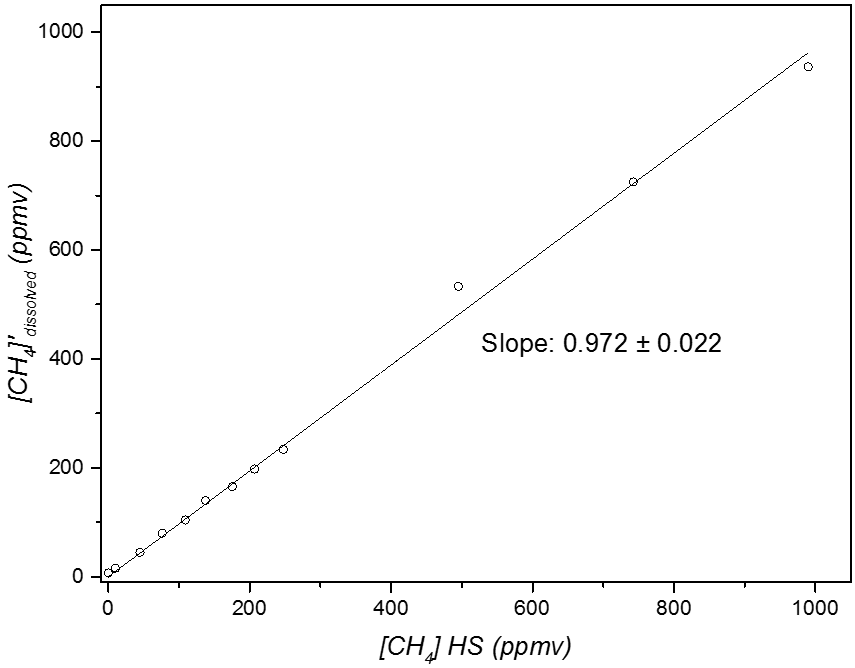

Figure 2.8: The calibration curve obtained before the campaign. The [CH_4] HS is the concentration measured at the head space while the [CH_4]'$_{dissolved}$ is the dissolved gas concentration measured by the sub-ocean instrument.

2.4.5. Measurements in Lake Kivu

During the campaign, a total of eight continuous profiles were recorded using the Sub-Ocean instrument. The optical spectrometer embedded in the sensor is designed for trace gas measurements and prior to the campaign its wavelength was tuned in order to access to very weak rotational-vibrational transitions in the near-IR region. Despite the efforts, the maximum achieved depth before saturation of the optical signal was 150 m, which is not ideal, but enough for comparing the results and proving the capability of the instrument to measure in such extreme conditions. The sensor was deployed during four days from 10 to 13 March 2018. Two profiles were recorded on the first day and two on the last. On 11 March, only one profile was recorded but discarded because of its quality, while on 12 March, the day were the campaign was focused on the deepest location of the lake, two profiles were recorded but CTD data were not stored by the device, and therefore depth information were missing for those two profiles. The pressure sensor embedded on the instrument that was installed in order to register water pressure and therefore depth did not function correctly during the campaign.

In Figure 2.9 an example of a single profile is reported. The sensor reached 100 m depth in 18 min. On the right-hand side, dissolved CH_4 measurement is plotted against depth for showing the reproducibility of the sensor during descent and ascent.

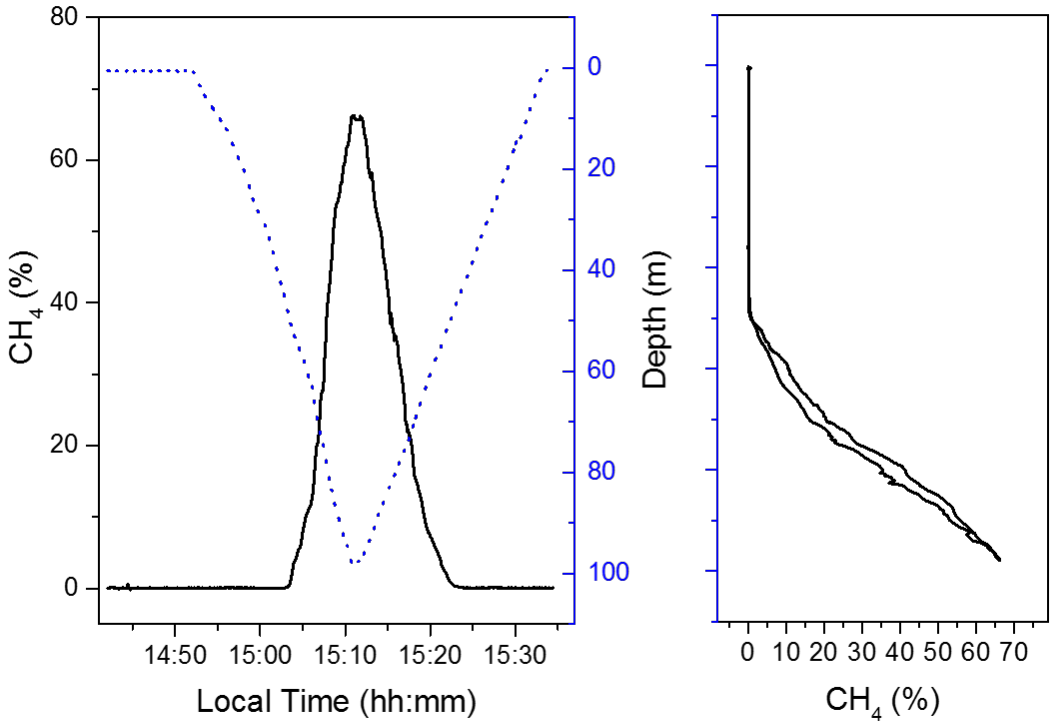

Figure 2.9: The second profile (P02) recorded on 10 March 2018. The 100 m downward and upward profile was recorded in 42 min. On the right panel the two profiles are superposed, highlighting the reproducibility of the measurement between descent and ascent.

Eight vertical profiles (downward and upward) were therefore used for the analysis. They are reported in Figure 2.10 together with CTD data (temperature, conductivity and dissolved oxygen). Only one of the eight profiles reached 150 m, while the others are shallower, only covering the first 100 m of depth. From the dissolved CH_4 data at 80 m depth, the precision of the measurement could be estimated, with an average concentration 35.53 ± 8.2%, corresponding to 508.3 ± 117 mbar of partial pressure and 0.71 ± 0.16 mmol L^{-1} of CH_4. The large standard deviation of 22 % of the measurement at 80 m depth can be explained by the large uncertainty in retrieving the flow of dry gas permeating the membranes. The same standard deviation was used as an estimate for the uncertainty of the measurements at all depths. In order to further increase the dynamic range of the sensor, during the last day of campaign one of the two membranes was removed and replaced with a Teflon sheet. This allowed increasing the dilution factor by a factor of two while adding the carrier gas, but leading to a decreasing by a factor of two of the dry flow at the membrane (which reached only ~0.065 cm^3 STP/min). The large uncertainty on this dry flow measurement directly affects the accuracy on the concentration. Nevertheless, the measurements with only one membrane allowed to displace further down in depth the saturation of the signal of the optical spectrometer, and acquire information on dissolved CH_4 down to 150 m.

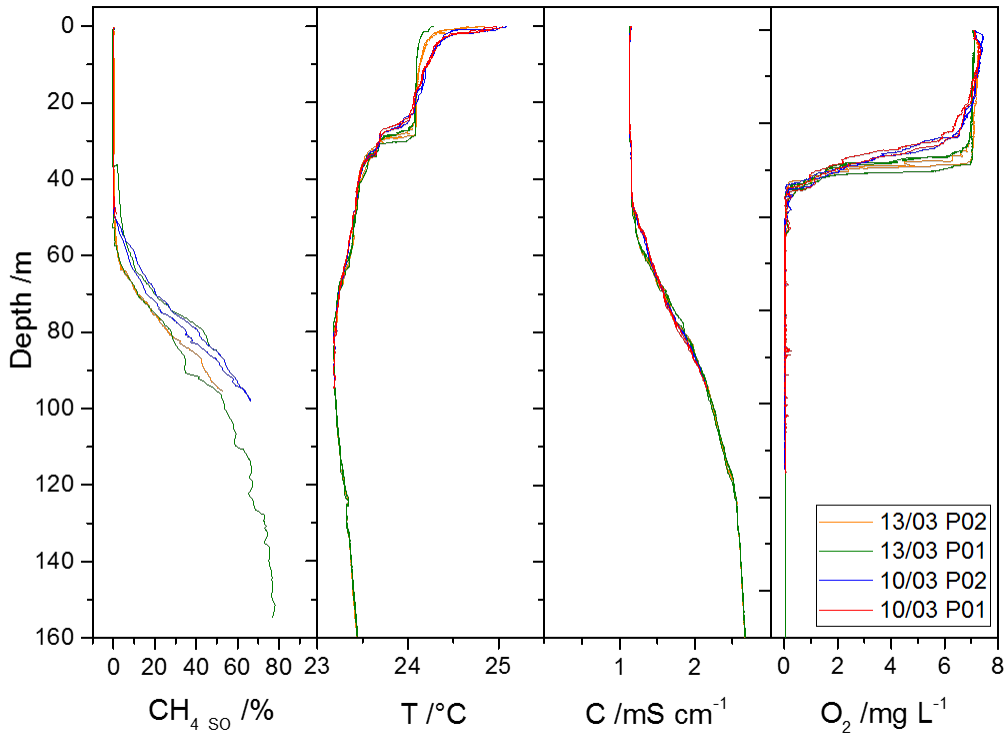

Figure 2.10: Dissolved methane data from the eight profiles used for the data analysis. Each coloured profile includes the downward and upward record. Temperature, conductivity and dissolved oxygen data from the CTD attached to the Sub-Ocean instrument are also reported.

2.4.6. Conversion from mixing ratios to concentrations

So far, concentrations are reported in unit of mixing ratio. This is because the spectrometer is measuring in the gas phase, and raw data are expressed as the concentration of CH_4 with respect to the amount of the total dry gas. As reported in equation (2) above, this technique requires to know the main composition of the dissolved gas, in order to account for the different permeation coefficients of the species through the silicon membrane. This is not a problem for most of the ocean and lake settings, where the gas mixture is mainly composed of nitrogen and oxygen, but more difficult for setting such as Lake Kivu. For the data analysis we assumed a bulk gas mainly composed of N_2, O_2, CO_2 and CH_4. Oxygen concentrations were calculated from the CTD measurements and converted into partial pressure using equation 19 from Sander 2015 (H^{cp} of 1.25 × 10^{-5} mol m^{-3} Pa^{-1} and $d\ ln(H^{cp})/d(1/T)$ of 1500 K). For CO_2, the profile from 2004 calculated from alkalinity and adjusted pH measurements by Schmid et al. (2005) was used. The O_2 and CO_2 profiles used for the analysis are reported in Figure 2.11.

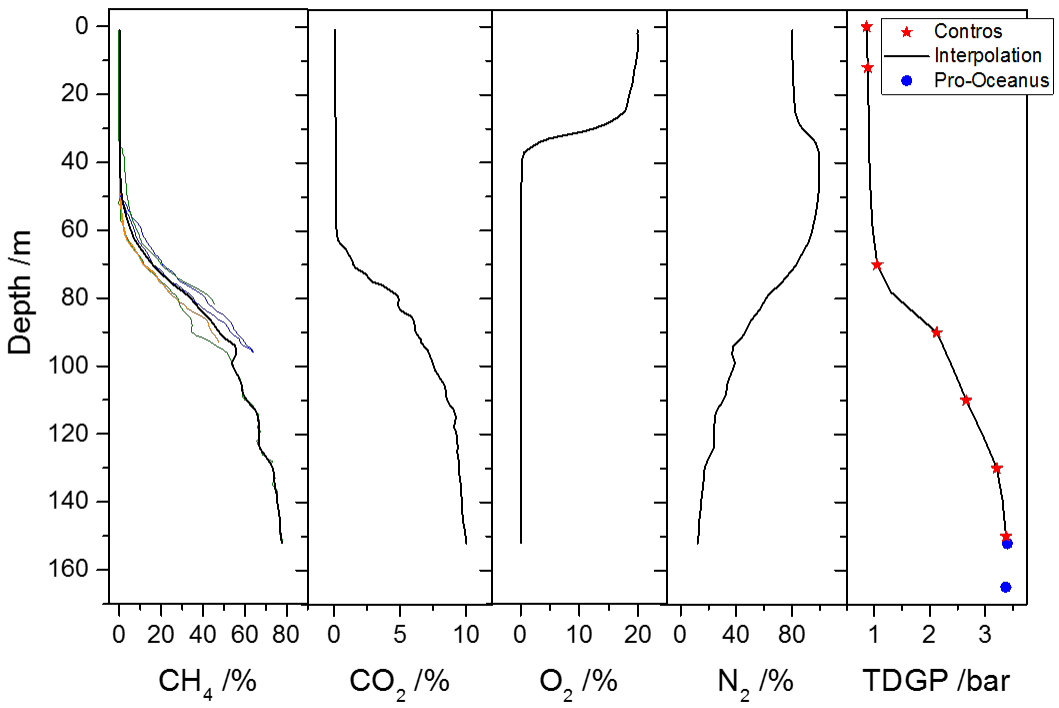

Figure 2.11: Mixing ratios of individual gas species in the main gas mixture and total dissolved gas pressure. Coloured CH_4 lines are the profiles also reported in Figure 2.10, while the black line is the averaged value. CO_2 data are from Schmid et al., 2005, O_2 are from CTD data during the campaign, and N_2 is the retrieved nitrogen concentration (TDGP – pCH_4 - pCO_2 - pO_2). For the TDGP, red stars were recorded by KivuWatt using Contros HydroC Sensors, the black line is an interpolation of the data and blue dots were recorded by UFZ using a Pro-Oceanus mini-TDGP sensor.

In order to convert the continuous profiles from mixing ratio into unit of partial pressure, information of total dissolved gas pressure (TDGP) is required. This information was extracted from the discrete profiles recorded by KivuWatt during this campaign using the HydroC Contros instrument. Since these instruments wait for equilibration across the semipermeable membrane, the pressure measured on the dry side of the membrane corresponds to the total gas content. The data are reported as red stars in Figure 2.11 and were interpolated in order to match the depth resolution of the continuous profile of Sub-Ocean (black line). During this campaign, TDGP data were also recorded by UFZ using the commercial mini-TDGP sensor (Pro-Oceanus) but only below 150 m. Two measurements from this dataset, at 152 and 165 m, have been reported as blue dots in Figure 2.11 showing a good agreement with the Contros data. TDGP data were used to convert CO_2 and O_2 data from partial pressure into mixing ratio (expressed in percentage). Finally, gas pressures were converted to gas concentrations using the method described in section 2.7.

2.5. In-situ sampling in gas bags combined with gas chromatography

These measurements were performed by UFZ Magdeburg.

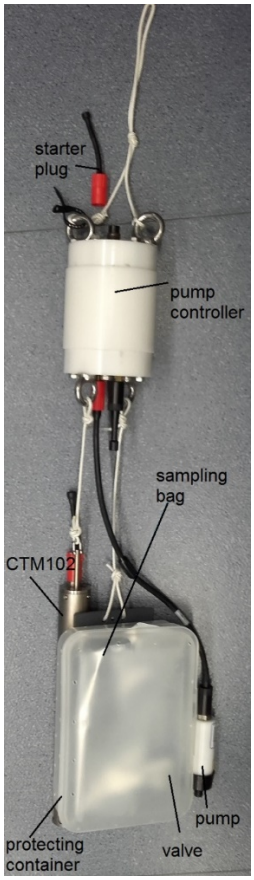

Figure 2.12: Gas sampling arrangement as used in Lake Kivu with pump controller, submersible pump, and protection housing for the sampling bag; a small CTD-probe was connected to record depth, electrical conductivity and temperature and started synchronously with the pump controller ("starter plug").

For gas measurements, gas tight sampling bags (TECOBAG; see Horn et al., 2017) were lowered to the investigation depths and partially filled with water by operating a pump for a short period (Figure 2.12). Enough remaining capacity of the bag was retained to accommodate the total amount of gas released when bags were recovered and thus pressure was reduced to atmospheric level. Other than in previous implementations of this technique in Lake Vollert-Sued, Germany (Horn et al., 2017) and Guadiana Pit Lake, Spain (Boehrer et al 2017) the pumps were switched on and off by a submersible controller. For all samplings, a CTD probe (Sea and Sun Technology; CTM102) accompanied the sampling equipment to measure the sampling depth accurately. 15 depths were sampled in March 2018, of which 2 had to be discarded due to a probably faulty gas volume measurement. In addition, 5 samples from a previous field campaign on 27th May and 2nd June 2017 were added to the analysis. The sampling method had especially been developed for extreme gas pressures, all samples were taken between 150 and 450 m depth.

Figure 2.13: Filled sampling bags in the field laboratory of LKMP and the gas chromatograph used for measuring the composition of the gas samples.

After filling, sampling bags were transported to the LKMP laboratory and left there over night to reach equilibrium between the gas phase and the dissolved phase. The mass of water was measured by weighing the bags on the weight scale of LKMP under consideration of the weight of the bags and the density of the water. The volume of the gas space was measured thereafter by withdrawal through syringes from the bags.

The composition of gases was detected with a gas chromatograph (GC, Perkin-Elmer Clarus 580) in the LKMP laboratory. Before measurements, the previous calibration of the instrument from 2017 was confirmed with a dry gas standard of composition 20 % N_2, 40 % CH_4, 40 % CO_2 at an accuracy of 0.7 % or better. Samples, however, were in contact with a water phase during equilibration. Hence, a certain portion of moisture was expected in the samples. The detected gases amounted to ~97 %; the undetected 3 % corresponded very well with the expected moisture at laboratory temperatures and hence were attributed to water vapour. The measured concentrations of CH_4 and CO_2 were multiplied by the gas volume to yield the amount in the gas space.

To determine the entire amount of CH_4 in the sample, the amounts of gases remaining dissolved in the water were calculated assuming equilibrium between the water and gas phase at temperature and pressure in the laboratory. As the gas volume was of the same order of magnitude as the water inside the bag, this contributed a few percent to the total amount of CH_4.

Due to its high solubility, a considerable portion of CO_2 remained in solution, and hence required a more accurate determination. Hence, only in the case of CO_2, the dependence of the Henry coefficient on electrical conductivity (of few percent in the considered range) was included in the calculation: based on electrical conductivity C_{25} at the sampling depth (see Figure 2.2) the Henry coefficient was interpolated between freshwater (C_{25} = 0 mS/cm) and seawater (C_{25} = 53 mS/cm) given by Murray and Riley (1971, see also Horn et al., 2017). In addition, the concentration of bicarbonate in the water phase was calculated based on pH-measurements in the laboratory by inserting a sensor after the volume and GC measurements

were completed. A dissociation constant of pK_1= 6.2 was used (Cai and Wang, 1998). Hence, we could evaluate the dissolved inorganic carbon DIC as the sum of three contributions: CO_2 in gas space, CO_2 dissolved in water, and HCO_3^-. CO_2 concentrations in the lake were calculated by adding the CO_2 gas volume in the sampling bag and the dissolved amount. The tiny contribution coming from bicarbonate shifting to dissolved CO_2 could be quantified (relative contribution of 10^{-5}) on the base of pH change from the field to the laboratory measurement. Hence it can be neglected without increasing the expected error.

The accuracy of the measurements was estimated from the following contributions: accuracy of volume measurement of gas 4 % (above 250 m 6 % due to smaller volume); Henry coefficients were known within 5 %, temperature fluctuations in laboratory allow for 5 % plus unknown variation of the Henry coefficient with Kivu-salts another 5 %; added as independent errors. This resulted in an 8 % error for the Henry coefficient. As less than half of the CO_2 remained in solution, this contributed less than 4 % to the expected error. In the case of CH_4, only a small fraction remained in solution, and the corresponding error contribution is less than 1 %. The error in the measurement of the mass (and volume) of the sample was smaller than 1 %. Altogether, we expected a precision of the measurement of 5 % for CH_4 (7 % above 250 m depth) and 6 % for CO_2 (8 % above 250 m). If required, the accuracy could be improved by implementing a better volume measurement of the gas. In the case of CO_2, a more exact knowledge of the Henry coefficient would help as well.

In conclusion, the sampling bags technique represents a simple approach, which requires careful sampling and a good understanding of the solubility of gases for the processing of data. Results are reliable, as the approach does not provide much space for hidden errors. Gas tight sampling bags for CH_4 and CO_2 are a precondition, which is very well accomplished for the investigated gases in the bags used.

2.6. Sampling with tubes combined with on-site mass spectrometry

These measurements were performed by the team from Eawag.

The measurement approach is schematically summarized in Figure 2.14. Lake water is pumped to the surface continuously using a 0.75 kW submersible centrifugal pump (UG-18 from Pumpen Lechner) down to a depth of 250 m. Below 250 m, no pump is needed because the outgassing of deep water in the tube sustains the water flow. However, a small peristaltic pump is used to initiate the process by bringing deep water close to the lake surface where the hydrostatic pressure is too low to keep the gases in the water. Relevant data about the pump operation above/below 250 m are shown in Table 2.4.

2.6.1. Overview

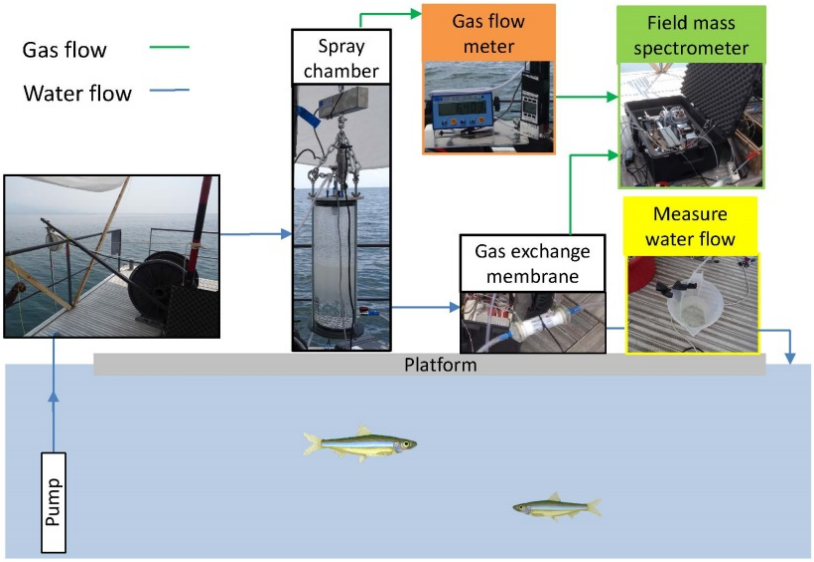

Figure 2.14: Sketch of measurement approach: lake water is pumped up continuously and dispersed into a spray chamber. The equilibrated gas and water phases flow out of the spray chamber at the top and bottom, respectively. For both phases, partial gas pressures and flows are measured.

A custom-made spray chamber (d = 12 cm, h = 40 cm, V = 4.5 L) is subsequently used to separate water and gas phase of the sampling water by dispersing it through a nozzle at the top. Gas and water phases leave the spray chamber through an outlet at the top and at the bottom, respectively. Pressure (Wika P-30, accuracy: 1 hPa) and temperature (Maxim DS18B20, accuracy: 0.5 °C) are recorded continuously for both gas and water while gas flow is measured using a laminar flow meter (Alicat Scientific MBS-20SLPM-D, accuracy: 2.5 to 8.5 % in the deep water) and water flow using a simple bucket. Finally, the gas phase components are directly analyzed in the field mass spectrometer. In order to quantify the remaining gas in the sample water, the headspace of a membrane module is equilibrated with the sampling water flowing from the spray chamber and also analyzed using the mass spectrometer.

Table 2.4: Pump operation data

	Pump	Tube	Flow	Tube flushed
Above 250 m	Yes	polyamide, 6 mm	ca. 1.6 L/min	2x
Below 250 m	No	polyamide, 10 mm	0.5 - 1 L/min	2x

There are two crucial components in the measurement approach: the portable field mass spectrometer, developed at Eawag (Brennwald et al., 2016, see next section) and the gas flow meter MBS-20SLPM-D made by Alicat Scientific. The gas flow meter forces the gas through a laminar flow element and records the pressure drop across the element. This pressure drop is a linear function of gas flow and thus directly allows the instrument to calculate the gas flow for a given gas mixture. The range of the instrument is from 0.1 to 20 l/min and its accuracy depends on the average flow measured (between 2.5 and 8.5 % in the deep water).

2.6.2. On-site mass spectroscopy

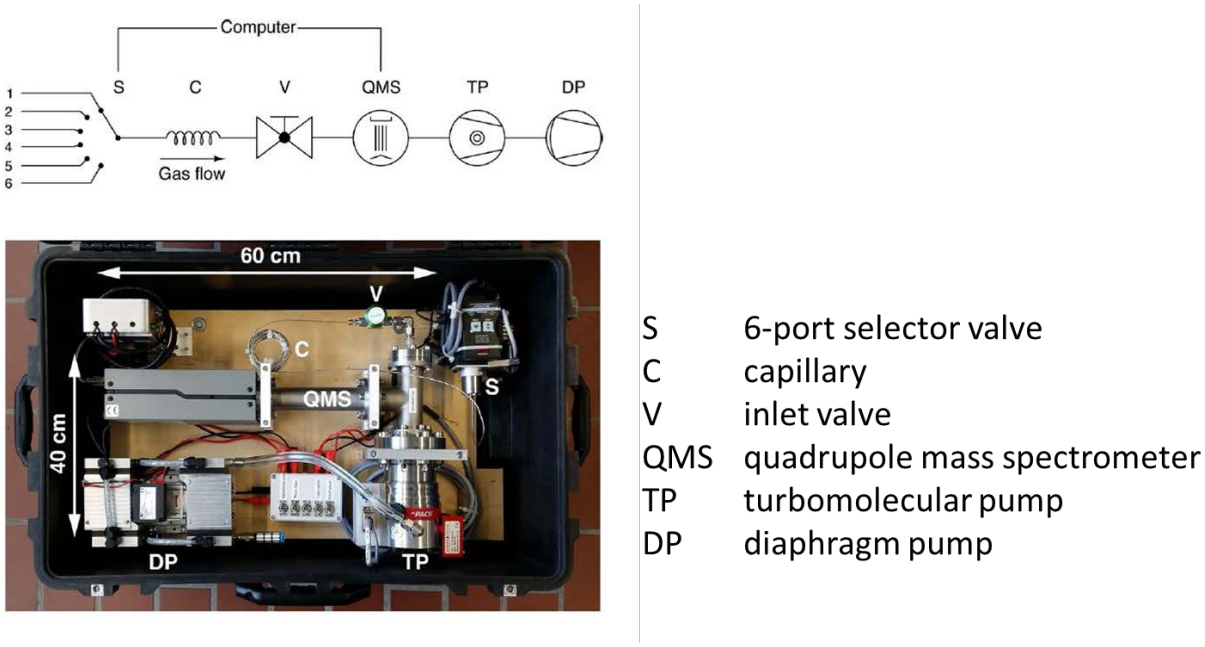

Figure 2.15: On-site mass spectrometer developed at Eawag (Brennwald et al., 2016)

Figure 2.15 shows the main components as well as sketch of the mass spectrometric system. Sample or calibration gas enters through one of the ports of the multi-port selector valve and enters the quadrupole mass spectrometer (QMS) through a long capillary. The QMS is evacuated using a low and a high vacuum pump and is suitable for the analysis of any gas between 0 and 200 atomic mass (atm).

If the sample medium is gas (e.g. the gas from deep water in Lake Kivu), the sample can directly enter the QMS. But if water is sampled (down to 130 m in Lake Kivu and for residual gas concentration in water below 130 m), the gas contained in the water needs to be extracted into a headspace. In our approach, this is done using a Liqui-Cel G542 membrane module. Ideally, the water flow through this membrane should be higher than ~0.5 L/min in order to guarantee an equilibrium in the headspace despite the slow consumption by the QMS. Using the equilibrium assumption, the gas concentration in the water can be deduced using the Henry coefficient, and membrane properties do not have to be taken into account.

The device was calibrated several times per day using the following calibration gases (contained in Linde Plastigas bags and permanently attached to two inlets):

- 20 % of CH_4, 80 % of CO_2
- 30 % of CH_4, 60 % of CO_2, 10 % of air

2.6.3. Calculations

In order to compute in-situ concentrations from concentrations in the gas and water phase, we use the following equation:

$$C_{in\ situ}\left[\frac{mmol}{L}\right] = \frac{Q_{gas}\left[\frac{L_{gas,SATP}}{min}\right]}{Q_{water}\left[\frac{L}{min}\right]} C_{gas}\left[\frac{mmol}{L_{gas,SATP}}\right] + C_{water}\left[\frac{mmol}{L}\right] \quad (4)$$

where C is concentration measured by the mass spectrometer and Q is flow. Q_{water} is measured using a bucket and Q_{gas} is the gas flow at standard ambient temperature and pressure SATP (T = 25°C and P = 1013 hPa) computed according to equation (5).

$$Q_{gas}\ \left[\frac{L_{gas,SATP}}{min}\right] = \frac{V_{out,SATP} + (M_{init} - M_{final}) 1\left[\frac{L}{kg}\right] \frac{P_{ambient}}{P_{SATP}}}{t}, P_{ambient} = 855\ hPa \quad (5)$$

$V_{out,SATP}$ is the total outflow volume (in $L_{gas,SATP}$) measured by the gas flow meter during the time t (min). M_{init} and M_{final} are the weight (kg) of the spray chamber at the start and at the end of a gas flow measurement (usually 20-30 minutes) which take into account the water level variation in the spray chamber. Finally, the pressure correction term ensures coherences with the output of the gas flow meter in SATP (the temperature correction being negligible).

After calibration, the mass spectrometer gives out relative partial pressure values for every major gas component (CH_4, CO_2, N_2 and O_2). Water vapor is not measured but taken into account assuming saturation and by calculating saturation pressure (atm) according to the following equation (Robinson, 1954):

$$\ln(pH_2O) = 24.4543 - 67.4509\left(\frac{100}{T}\right) - 4.8489\ln\left(\frac{T}{100}\right) - 0.000544S \quad (6)$$

where T (K) is water temperature, and S (‰) is salinity, which is calculated from conductivity and ionic composition (Wüest et al., 1996). Finally, the relative pressures are converted to absolute pressures using pressure gauges at the inlet of the mass spectrometer.

The partial pressures are subsequently converted to concentrations. For the pure gas phase coming out of the spray chamber, this is done using the molar volume at SATP (25°C and 1013 hPa) in order to get the concentration in $\left[\frac{mmol}{L_{gas,SATP}}\right]$. For the water phase, we use the Henry coefficients for CH_4 (Yamamoto, 1976) and CO_2 (Weiss 1974) which results in concentration in $\left[\frac{mmol}{L}\right]$.

2.6.4. Accuracy

We first assess the accuracy of the individual concentration and flow measurements in order to conclude on the total uncertainty of our approach.

Mass spectrometer

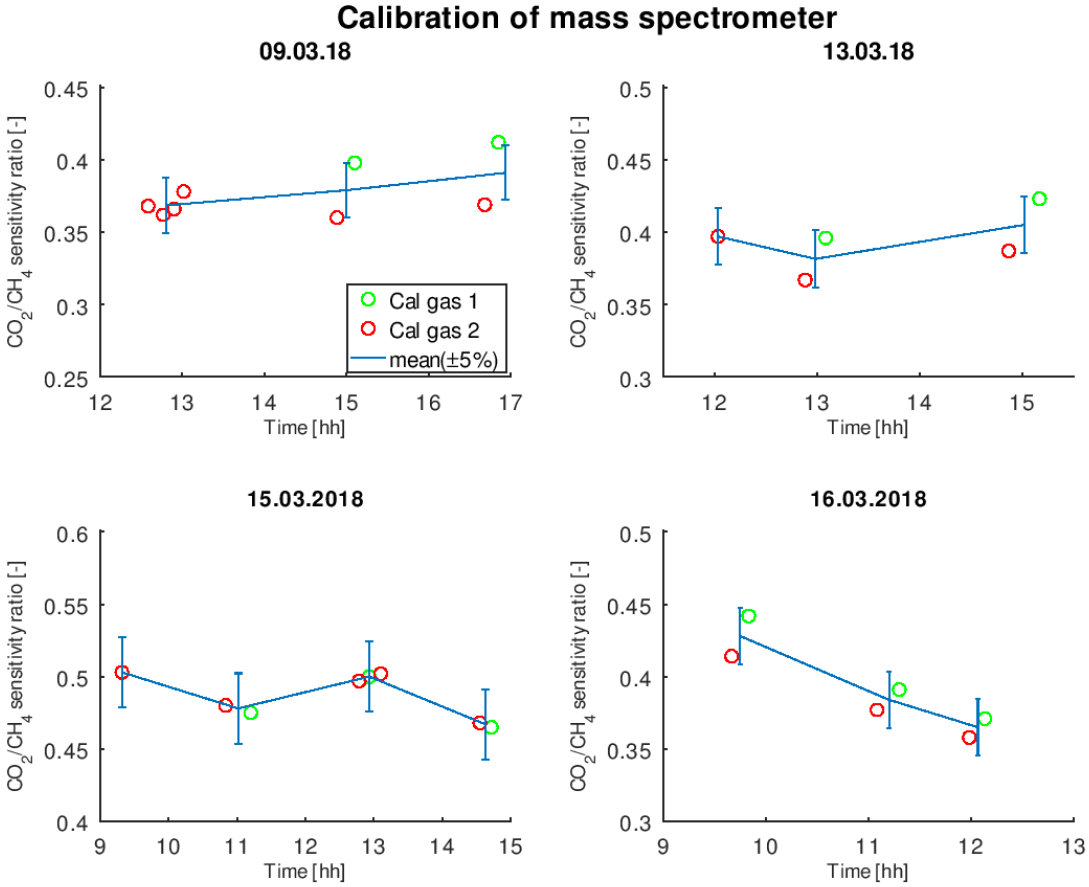

Figure 2.16: Variability of CO_2 to CH_4 sensitivity ratio of two different calibration gases for different measurement days. The sensitivity ratio of a gas is defined as the signal strength in [A] divided by its partial pressure in the calibration gas in [hPa].

Figure 2.16 depicts the CO_2/CH_4 sensitivity ratio for two different calibration gases (see section 2.6.2 for the composition of the gases) over several measurement days (most deep water samples were taken on these days). The sensitivity of a gas is given by the detector signal in Ampère divided by its partial pressure in the calibration gas mixture [A/hPa]. On 9, 13 and 16 March, the sensitivity ratio was significantly higher for calibration gas 1 than for calibration gas 2. However, no clear indication was found to discard any of the two calibration gases and therefore both gases were used for calibration purposes. The corresponding uncertainty range of the sensitivity ratio was estimated to 10 % resulting in a deviation of ± 5 % from the mean value (blue error bars in Figure 2.16).

In the following, the individual uncertainties of the CH_4 and CO_2 measurements are estimated from the uncertainty of the sensitivity ratio *E(CO_2_sens/CH_4_sens) = ± 5 %,* where E(…) means uncertainty.

The sensitivities are obtained by dividing the calibration signal [A] by the partial pressure in the calibration gas [hPa]. The calibration signals for both CO_2 and CH_4 (and their uncertainties) are not related to each other. Thus, assuming that CH_4 and CO_2 have the same relative uncertainty, we get *E(CO_2_sens) = E(CH_4_sens) = ± 2.5 %* (from uncertainty propagation of the ratio of two independent variables for small uncertainty).

To obtain the raw result of a sample, CH_4_sens is multiplied by "CH_4_signal" which is the signal measured at a certain depth in [A]. This raw result is called "CH_4_meas". The uncertainty of CH_4_signal due to the variability of the individual mass peak measurements is *± 1 %*. Therefore, *E(CH_4_meas) = E(CH4_sens) + E(CH_4_signal) = 2.5 % + 1 % = ± 3.5 %.* The same is valid for CO_2.

The final result consists of the measured quantity normalized by the ratio of total pressure (uncertainty around 0.1 % which is neglected here) and total gas pressure found by the mass spectrometer which is almost equal to CO_2_meas + CH_4_meas below 250 m: *E(CH_4_result) = E(CH_4_meas/(CH_4_meas + CO_2_meas))* and *E(CO_2_result) = E(CO_2_meas/(CH_4_meas + CO_2_meas))*. The denominator of these equations not only depends on the error of both CH_4_meas and CO_2_meas but also on the ratio of these measured values. Additionally, nominator and denominator are not independent, thus making a general assessment difficult. Thus, we proceed with the calculation of "extreme" cases (all errors add up) and we find for a typical CH_4/CO_2 ratio of 0.2/0.8 = 0.25:

E(CH_4_result) ≅ ± 5.5 %

E(CO_2_result) ≅ ± 1.5 %

The ratio of these errors is around 4 because at the given composition of the gas phase, a 1 % increase in CO_2 concentration roughly results in a 4 % decrease in CH_4 concentration.

Henry coefficient

In the case of CO_2, a large fraction of the gas remains dissolved in the sample water. For determining its concentration, the measured partial pressure is multiplied by the temperature-dependent Henry coefficient. Our temperature sensor has an accuracy of 0.5°C which leads to an additional error of 1 %. We adopt a total uncertainty of 3 % to account for the uncertainty of the temperature-dependence of the Henry coefficient and for the fact that the equilibrium in the membrane contactor might not be perfect.

For CH_4, the uncertainty in the Henry coefficient can be neglected, since only a small fraction of the gas remains in the water after degassing.

Gas flow

The gas flow is computed using equation (5). According to the manufacturer, the accuracy of the total gas volume $V_{out,SATP}$ which passed through the gas meter in time t is given by

$$\Delta_{V_{out,SATP}}[\%] = \frac{0.8\%\frac{V_{out,SATP}}{t} + 0.2\% Q_{Full\ scale}}{\frac{V_{out,SATP}}{t}}\ ,\ Q_{Full\ scale=20\ L/min} \quad (6)$$

This error is between 2.5 and 8.5 % in the deep water due to the high full scale value of the gas meter. Thus the contributions of the hanging scales and the pressure gauge (both 0.1 % accuracy) are negligible in comparison and we can state

$$\Delta_{Q_{gas}} = \Delta_{V_{out,SATP}} = 2.5 - 8.5\ \% \quad (7)$$

Water flow

We used a 5 L bucket with labelling every 50 mL, usually filled to 3 to 4 L. Experiments in the laboratory show a positive bias of 3 % and random fluctuations of ± 1 % (Figure 2.17). The positive bias was corrected by multiplying the measured water flow by 0.97. We estimated the accuracy of the corrected water flow to be ± 1 %.

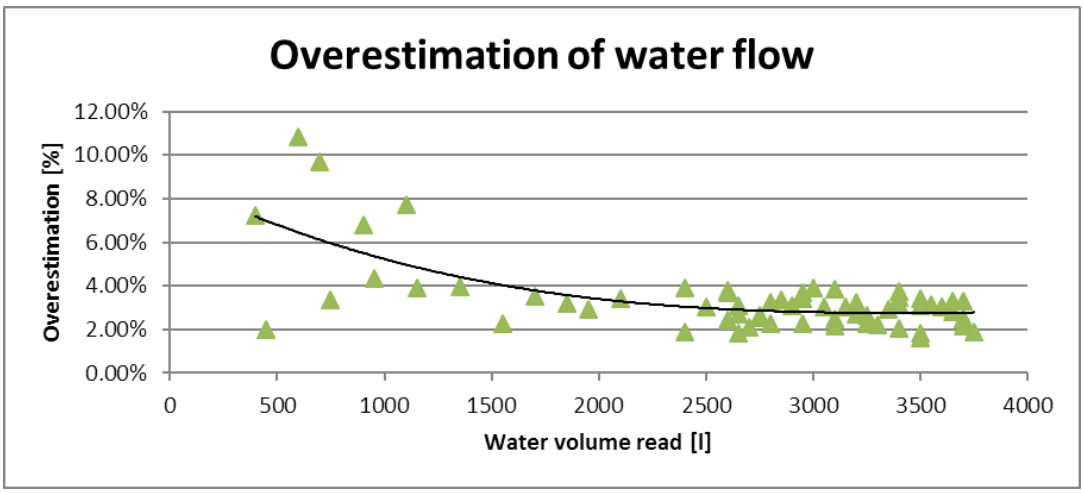

Figure 2.17: Bias and uncertainty of water flow measurement

Total accuracy

We estimated the individual accuracies above, so the true values of the individual measurements (Q_{gas}, Q_{water} and MS measurement) should lie within those limits. In the worst case, we will either underestimate or overestimate the true value of all those individual measurements at the same time. Assuming that all individual errors are small, the maximum uncertainty of the gas amount contained only in the gas phase is given by the sum of the relative errors. We give here an example for the calculation of the uncertainty of CH_4 and CO_2 at 410 m depth.

CH_4:

$$\Delta_{CH_4} = \Delta_{Q_{gas}} + \Delta_{Q_{water}} + \Delta_{Conc.} = 9.2\ \% \qquad \Delta_{Q_{gas}} = 2.7\ \%,\ \Delta_{Q_{water}} = 1\ \%,\ \Delta_{Conc.} = 5.5\ \% \quad (8)$$

This means that in the worst case, the true value in the gas phase is under- or overestimated by around 9 %. The error contribution from the CH_4 remaining in the water phase is neglected as it is around 1 % of the total CH_4.

CO_2:

The uncertainty of the CO_2 measurement is a weighted sum of the uncertainties in the gas and water phase respectively

$$\Delta_{CO_2\_gas} = \Delta_{Q_{gas}} + \Delta_{Q_{water}} + \Delta_{Conc.} = 5.2\ \% \qquad \Delta_{Q_{gas}} = 2.7\ \%,\ \Delta_{Q_{water}} = 1\ \%,\ \Delta_{Conc.} = 1.5\ \% \qquad (9)$$

$$\Delta_{CO_2\_water} = \Delta_{Conc.} + \Delta_{\mathrm{Henry}} = 4.5\ \% \qquad \Delta_{Conc.} = 1.5\ \%,\ \Delta_{Henry} = 3\ \% \qquad (10)$$

Therefore, the accuracy of CO_2 is the weighted average of equations (9) and (10) (closer to equation (9) in the deep water and almost equal to equation (10) at the surface).

Below 250 m, the uncertainty of CH_4 is in general around 10 % while that for CO_2 is on the order of 5 %.

2.7. Conversion between partial pressures and dissolved gas concentrations

In-situ measurements of partial gas pressures need to be converted to dissolved concentrations to compare them with direct observations of dissolved gas concentrations and to calculate the total gas content in the lake. For all calculations in this section we approximate the density of water at atmospheric pressure to be 1 kg L^{-1}, which is correct for the conditions in Lake Kivu within 2 ‰ (Schmid et al., 2004). Correspondingly, molar concentrations (expressed in mol L^{-1}) are assumed to be equal to molal concentrations (expressed in mol kg^{-1}).

The dissolved concentration C_i of a gas i can be calculated from its partial pressure p_i using the following equation:

$$C_i = K_i(T, S, P) p_i \varphi_i(T, P) \qquad (11)$$

where φ_i is the fugacity coefficient, i.e., the ratio between the fugacity of a gas and its partial pressure, which is a function of temperature *T* and pressure *P*, and K_i is the solubility coefficient, i.e., the ratio between the dissolved concentration of a gas and its fugacity. The calculation is done in the following steps:

1) Calculation of the solubility coefficients

The solubility coefficients K_i (mol L^{-1} atm^{-1}) of CO_2 and CH_4 as a function of temperature T (K) and salinity S (g/kg) are calculated using the following equation:

$$ln(K_i) = A_1 + A_2(100/T) + A_3 \ln(T/100) + S[B_1 + B_2(T/100) + B_3(T/100)^2] \qquad (12)$$

For CO_2, according to Weiss (1974), the parameters in equation (12) take the following values: A_1 = -58.0931, A_2 = 90.5069, A_3 = 22.2940, B_1 = 0.027766, B_2 = -0.025888, B_3 = 0.0050578.

For CH_4, the respective values are taken from Wiesenburg and Guinasso (1979): A_1 = -71.9959, A_2 = 101.4956, A_3 = 28.7314, B_1 = -0.076146, B_2 = 0.043970, B_3 = -0.0068672. In the original publication by Wiesenburg and Guinasso (1979), A_1 is given as -68.8862. The reason for this difference is that they expressed the dissolved concentration as a dimensionless value, i.e., volume of gas at standard conditions (STP; 0°C, 1 atm). At standard conditions, one mole of gas has a volume of 22.414 L. Therefore, their coefficient needs to be divided by 22.414 to convert it to mol L^{-1}. This is equivalent to subtracting 3.1097 from the parameter A_1 in equation (12).

Furthermore, the dependence for salinity in equation (12) has been derived for sea salt. The dissolved salts in Lake Kivu mainly consist of bicarbonates of Na, Mg, K, and Ca. We assume that the salinity effect depends mainly on the ionic strength of the solution. For seawater, the ionic strength I (mol/kg) can be calculated from unitless (i.e., kg/kg) salinity as $I = C_2*S/(1-S)$ (IOC et al., 2010) with C_2 = 19.8272 mol/kg. Since both the salinity correction of the Henry coefficient and the ionic strength in Lake Kivu are small, we can neglect the denominator and replace S in equation (12) by 1000 g/kg * I/C_2. The ionic strength in Lake Kivu was calculated as a function of conductivity, based on the observed average concentrations of the main dissolved ions and conductivities given in Tables 2 and 3 of Ross et al. (2015). A linear regression forced through the zero point resulted in an equation of $I = C_3\ \kappa_{25}$ (R^2 = 0.985), where κ_{25} (mS/cm) is the conductivity corrected to a standard temperature of 25 °C, and C_3 = 0.0173 (mol/kg)/(mS/cm). In summary, this results in the following equation for the Henry coefficients of CO_2 and CH_4 in Lake Kivu:

$$ln(K_i) = A_1 + A_2(100/T) + A_3\, ln(T/100) + C_1\kappa_{25}[B_1 + B_2(T/100) + B_3(T/100)^2] \qquad (13)$$

where $C_1 = 1000*C_3/C_2$ = 0.8725 (g/kg)/(mS/cm). Altogether, water with a conductivity of 1 mS/cm in Lake Kivu has about the same ionic strength as seawater with a salinity of 0.8725 g/kg.

Finally, it should be noted that for CO_2, this Henry coefficient is the ratio between the fugacity of CO_2 and the concentration of the dissolved undissociated aqueous CO_2, often referred to as H_2CO_3. For calculating the total dissolved CO_2, the concentration of bicarbonate (HCO_3^-) and carbonate (CO_3^{2-}) would have to be added.

2) Correction of the solubility coefficients for pressure

The solubility coefficients need to be corrected for the local pressure P (bar) at the sampling depth (sum of hydrostatic pressure plus atmospheric pressure), using the following equation (Weiss, 1974).

$$K_i(P) = K_i e^{\left[\frac{(1-P)vi}{RT}\right]} \qquad (14)$$

where R = 83.1446 cm^3 bar K^{-1} mol^{-1} is the gas constant, and vi are the partial molar volumes (cm^3 mol^{-1}) of CO_2 and CH_4. The partial molar volume of CO_2 was assumed to be constant at 32.3 cm^3 mol^{-1} (Weiss, 1974).

The partial molar volume of CH_4 was calculated from (Rettich et al., 1981):

$$v_{CH4} = e^{(3.541+0.00123(T-273.15))} \qquad (15)$$

The pressure correction factors ($K_i(P)/K_i$) range between 1 at atmospheric pressure and 0.93 (CO_2) or 0.94 (CH_4) at 50 bar, i.e., the local pressure reduces the solubility coefficient of the gases by 6 to 7 % in the lowest layers of Lake Kivu.

3) Fugacity coefficients

The fugacity coefficients were calculated using the methods described by (Ziabakhsh-Ganji and Kooi, 2012). A Maple script was provided by Z. Ziabakhsh-Ganji, which was transcribed to Matlab by M. Schmid. The script calculates among other things the fugacity coefficients for CO_2 and CH_4, including the interactions between both gases.

3. Analytical results - Methane concentrations

3.1. In-situ gas pressures using a Contros in-situ sensor

The partial pressures of CH_4 measured by KivuWatt using the method described in section 2.3 are presented in Table 3.1. The partial pressures were converted to CH_4 concentrations using the method described in section 2.7. The calculated concentrations are shown in Table 3.1 and Figure 3.1.

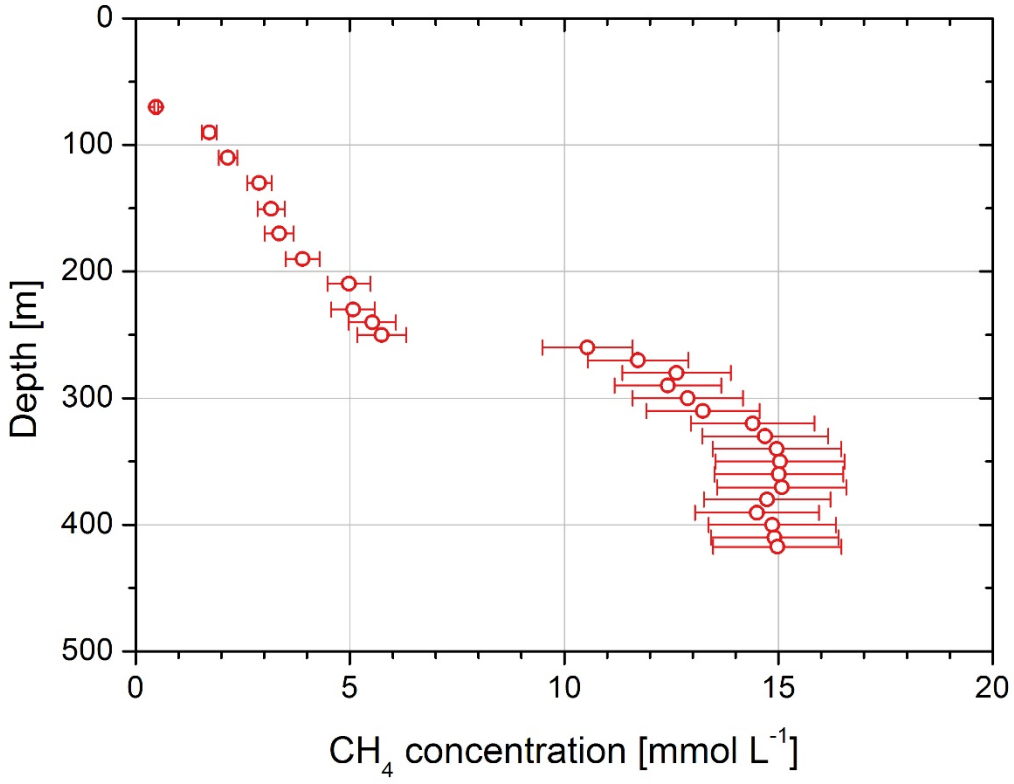

Figure 3.1: Methane concentrations and their uncertainties against depth in Lake Kivu calculated using the conversion method described in section 2.7. from gas pressures measured by KivuWatt with an in-situ nondispersive infrared absorption spectrometry sensor.

Table 3.1: Partial pressures of the dissolved methane measured by KivuWatt with an in-situ nondispersive infrared absorption spectrometry sensor as well as methane concentrations calculated from these partial pressures using the method described in section 2.7. The uncertainties shown here correspond to the estimated 10 % uncertainty for the measured partial gas pressure, and do not include a possible additional uncertainty of the conversion from partial pressure to concentration.

Depth (m)	CH_4 pressure (mbar)	CH_4 concentration (mmol L^{-1})	Uncertainty of CH_4 concentration (mmol L^{-1})
70	340	0.48	0.05
90	1246	1.72	0.17
110	1571	2.15	0.22
130	2134	2.89	0.29
150.5	2361	3.16	0.32
169.9	2523	3.35	0.34
190	2968	3.90	0.39
209.6	3845	4.98	0.50
230	3948	5.08	0.51
240	4323	5.52	0.55
250	4514	5.74	0.57
260	8442	10.55	1.05
270	9467	11.72	1.17
280	10263	12.62	1.26
290	10130	12.42	1.24
300	10562	12.89	1.29
310	10923	13.24	1.32
320	11986	14.40	1.44
330	12293	14.69	1.47
340	12590	14.96	1.50
350	12698	15.04	1.50
360	12720	15.01	1.50
370.5	12833	15.08	1.51
380	12572	14.74	1.47
390.5	12417	14.50	1.45
400	12783	14.84	1.48
410	12877	14.91	1.49
417.5	12969	14.97	1.50

3.2. In-situ methane concentrations using a Sub-Ocean prototype sensor

The CH_4 concentrations measured by CNRS using the method described in section 2.4 are presented in Figure 3.2.

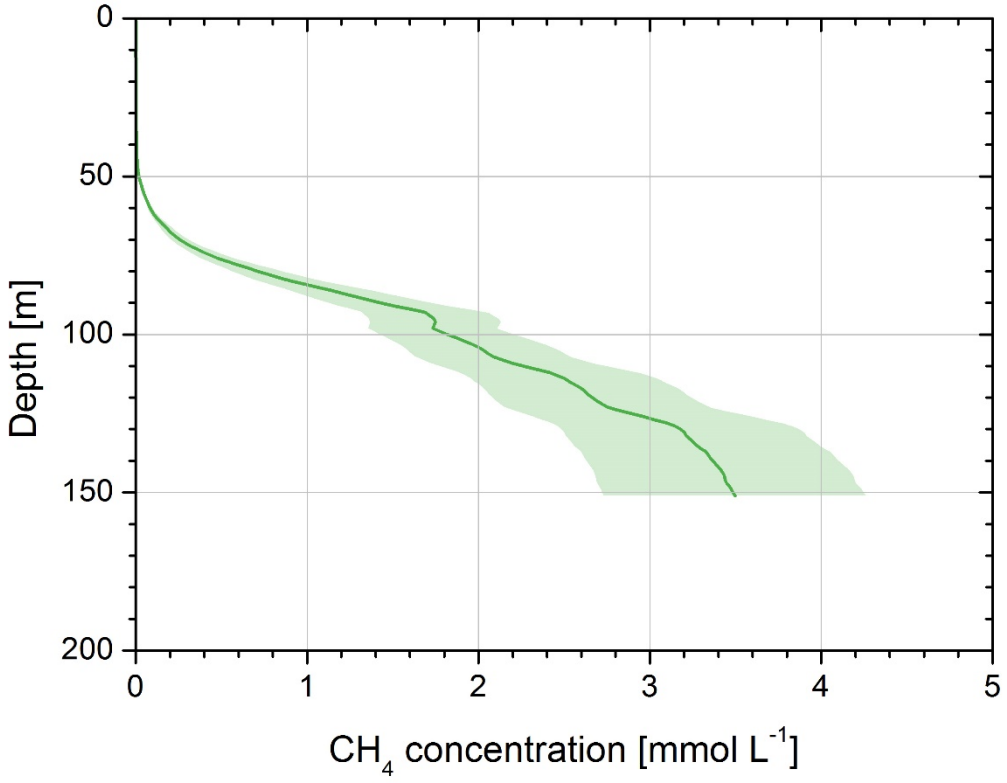

Figure 3.2: Continuous methane profile of the first 150 m of depth in Lake Kivu measured by CNRS with an in-situ sensor using laser spectrometry. Concentrations are plotted against depth. The shaded area indicates the estimated uncertainty of ± 22 %.

3.3. In-situ sampling in gas bags combined with gas chromatography

The CH_4 concentrations measured by UFZ using the method described in section 2.6 are presented in Table 3.2 and Figure 3.3.

Table 3.2: Methane concentrations in Lake Kivu and their estimated uncertainties measured by UFZ from samples taken with in-situ sampling bags. Depths marked with asterisks were sampled in May/June 2017.

Depth (m)	CH_4 concentration (mmol L^{-1})	Uncertainty of CH_4 concentration (mmol L^{-1})
150.6*	3.36	0.24
164.0	3.69	0.26
182.4	3.24	0.23
201.9	4.88	0.34
221.6	4.79	0.34
240.2	4.42	0.31
250.6*	6.22	0.44
259.8	11.81	0.59
280.4	13.94	0.70
292.3*	14.09	0.70
299.0	13.90	0.70
318.2	15.48	0.77
358.1	16.59	0.83
359.7*	17.19	0.86
377.9	16.54	0.83
397.0	16.73	0.84
411.7*	17.31	0.87
431.4	17.92	0.90

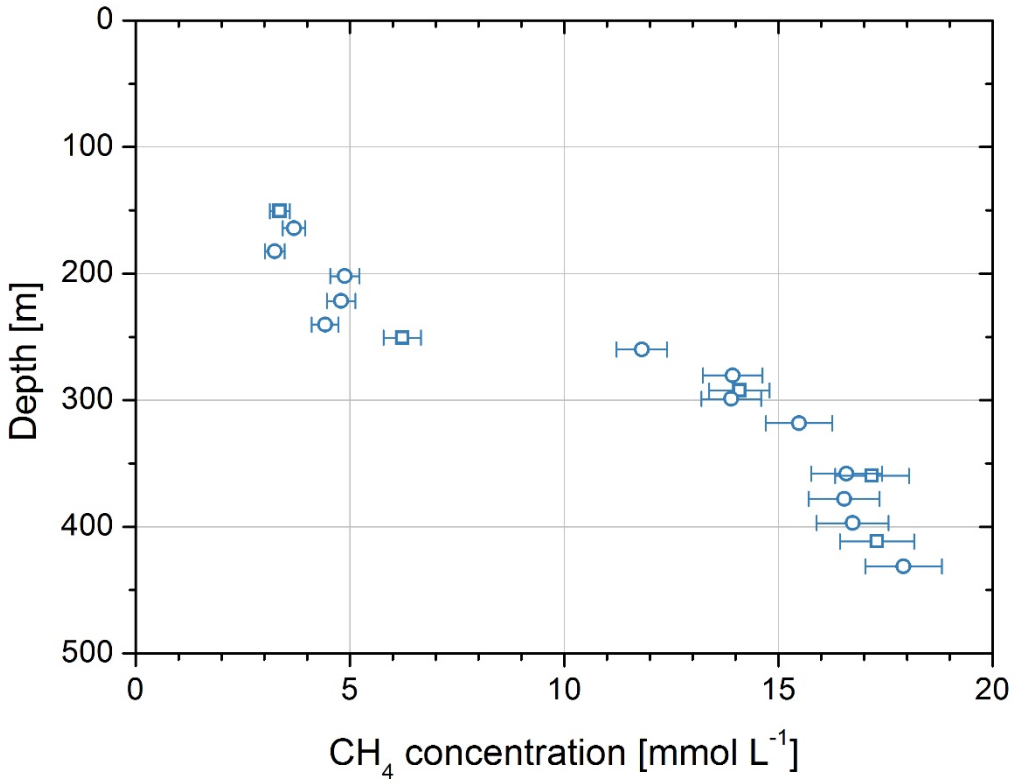

Figure 3.3: Methane concentrations and their uncertainties against depth in Lake Kivu measured by UFZ from samples taken with in-situ sampling bags. Samples were acquired in May/June 2017 (squares) and March 2018 (circles). Most of the samples were taken at Site 1, only the deepest measurement originates from sampling at Site 2.

3.4. Sampling with tubes combined with on-site mass spectrometry

The CH_4 concentrations measured by Eawag using the method described in section 2.6 are presented in Table 3.3 and Figure 3.4. Measurements in the depth range between 90 and 130 m were discarded, because at these depths, the water was already outgassing when brought to the surface, but the amounts of exsolved gas were too small for gas flow measurement. Concentrations in the top 50 m were below the detection limit of the system.

Table 3.3: Methane concentrations and their uncertainties measured by Eawag in Lake Kivu on 9-18 March 2018 using sampling tubes combined with on-site mass spectrometry.

Depth (m)	CH_4 concentration (mmol L^{-1})	Uncertainty of CH_4 concentration (mmol L^{-1})
11.2	<0.1	nA
31.7	<0.1	nA
50.4	<0.1	nA
71.3	0.47	0.03
151.7	3.70	1.06
171.8	3.24	1.00
191.7	3.96	0.90
212.1	5.42	0.96
241.7	4.85	0.71
254.4	6.60	0.79
269.6	14.97	2.29
289.2	13.50	1.65
308.7	16.23	1.92
335.2	16.93	1.64
354.9	17.09	1.66
374.7	17.49	1.78
394.3	16.51	1.63
414.2	17.24	1.62
453.0	16.73	1.57

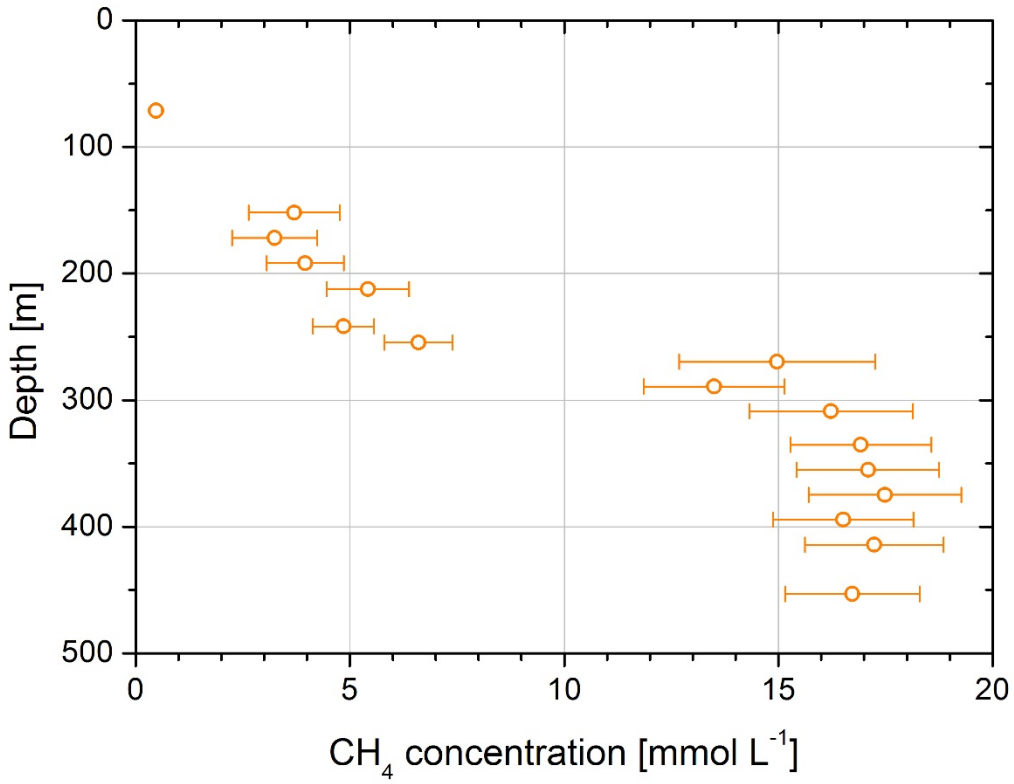

Figure 3.4: Methane concentrations and their uncertainties measured by Eawag in Lake Kivu on 9-18 March 2018 using sampling tubes combined with on-site mass spectrometry.

3.5. Comparison of methane concentrations with different methods

Figure 3.5 shows a summary of all CH_4 concentrations measured in this inter-calibration campaign. In general, there is a good agreement between the different methods. The main difference was observed below the main gradient, the UFZ and EAWAG concentrations showing slightly higher values than the KivuWatt Contros concentrations.

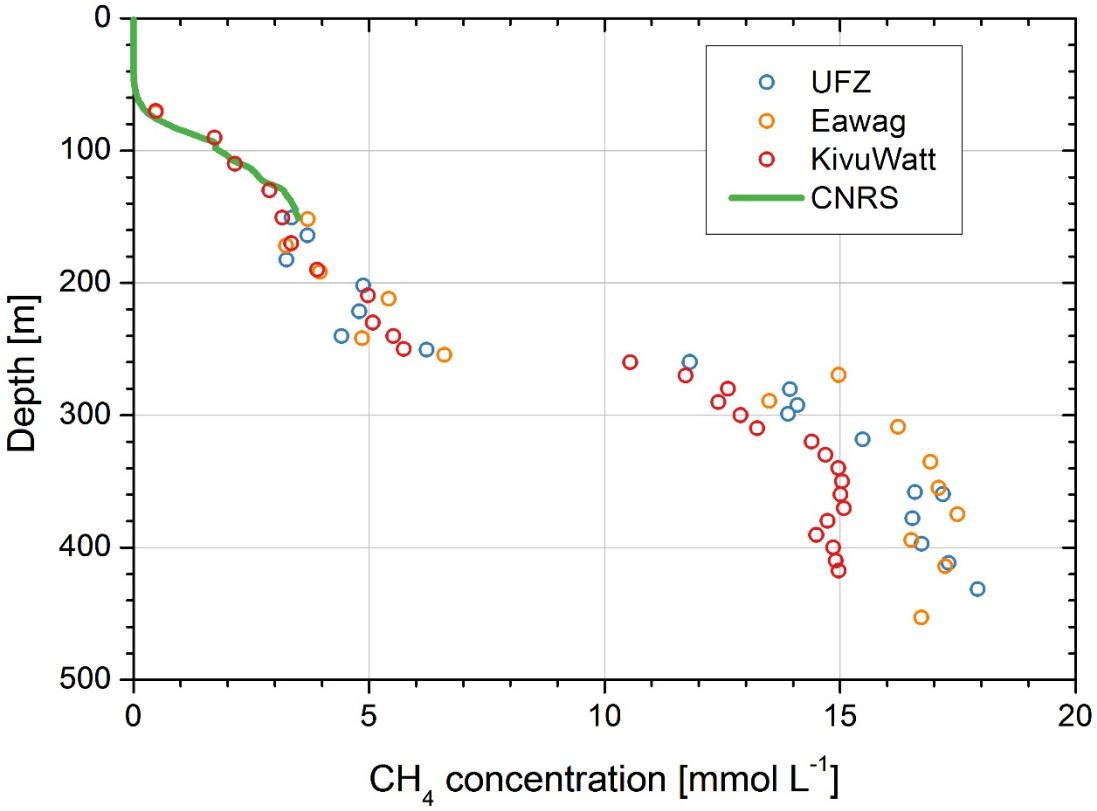

Figure 3.5: Summary of methane concentrations measured in the intercalibration campaign.

For estimating the gas content in the lake, a smooth curve of CH_4 concentrations with depth needs to be derived from the discrete measurements presented above. Since the transport processes in the lake, with a combination of slow upwelling and double-diffusive transport, are similar for all dissolved substances (Schmid and Wüest, 2012), and due to the very large residence times of CH_4 and dissolved substances of several 100 years in the lake, it is likely that the conductivity in the lake is related to the gas concentrations. The advantage of using conductivity (corrected to a temperature of 25 °C) as a proxy is that it can be very accurately measured with high vertical resolution. The following procedure was applied to derive smooth curves individually for the CH_4 concentrations measured by UFZ, Eawag (between 150 and 480 m depth) and KivuWatt (between 70 and 480 m depth):

We first extended the conductivity profile from Figure 2.2 down to 480 m depth with the background conductivity profile published by Ross et al. (2014). The latter was corrected with the mean difference between the two profiles in their lowest common 20 m. Conductivity was then sampled from this profile at the depths of the available gas measurements, and a polynomial function of 6th order was fitted (R^2 > 0.993 for all three datasets) with conductivity as the independent and gas concentrations as the dependent variable. The regression was used to compute the gas concentration as a function of conductivity and to relate it to depth.

Figure 3.6 shows the estimated smoothed CH_4 concentrations as a function of depth compared to the observations. These smoothed lines are used in section 6.3 to estimate the CH_4 stored in the lake. The smoothed UFZ and EAWAG concentrations are on average higher by 12 % and 16 %, respectively, than the KivuWatt Contros concentrations between 260 and 420 m depth. This difference is close to the upper limit but still within what would be expected from the estimated uncertainties of the individual methods. Part of the discrepancy could be due to uncertainties in the conversion of the KivuWatt data from partial pressures to concentrations.

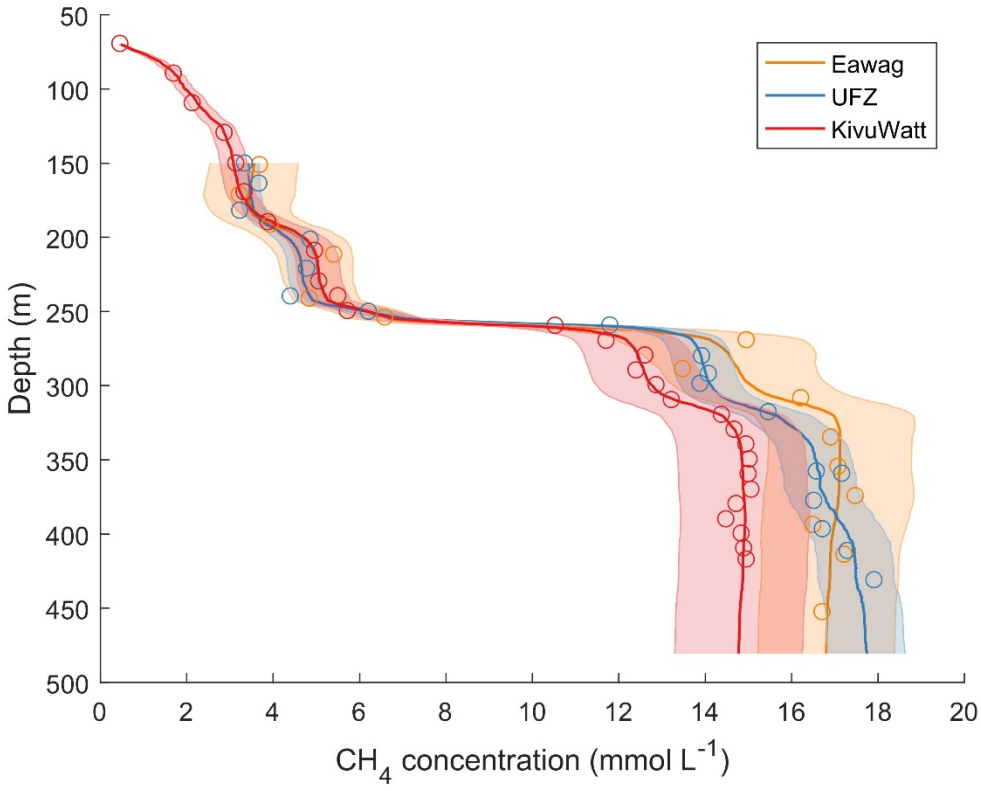

Figure 3.6: Smoothed methane concentrations compared to concentrations measured by UFZ, Eawag, and KivuWatt. The shaded areas indicate approximate error ranges (interpolated relative errors between data points) around the smoothed lines.

4. Analytical results – Carbon dioxide concentrations

4.1. In-situ sampling in gas bags combined with gas chromatography

The CO_2 concentrations measured by UFZ using the method described in section 2.6 are presented in Table 4.1 and Figure 4.1.

Table 4.1: CO_2 concentrations in Lake Kivu and their estimated uncertainties measured by UFZ from samples taken with in-situ sampling bags. Depths marked with asterisks were sampled in May/June 2017.

Depth (m)	CO_2 concentration (mmol L^{-1})	Uncertainty of CO_2 concentration (mmol L^{-1})
150.6*	11.42	0.91
164.0	11.86	0.95
182.4	13.26	1.06
201.9	20.61	1.65
221.6	21.41	1.71
240.2	21.52	1.72
250.6*	27.88	2.23
259.8	53.52	3.21
280.4	63.21	3.79
292.3*	64.99	3.90
299.0	64.21	3.85
318.2	72.93	4.38
358.1	84.68	5.08
359.7*	86.97	5.21
377.9	86.25	5.17
397.0	89.35	5.36
411.7*	92.24	5.53
431.4	93.76	5.63

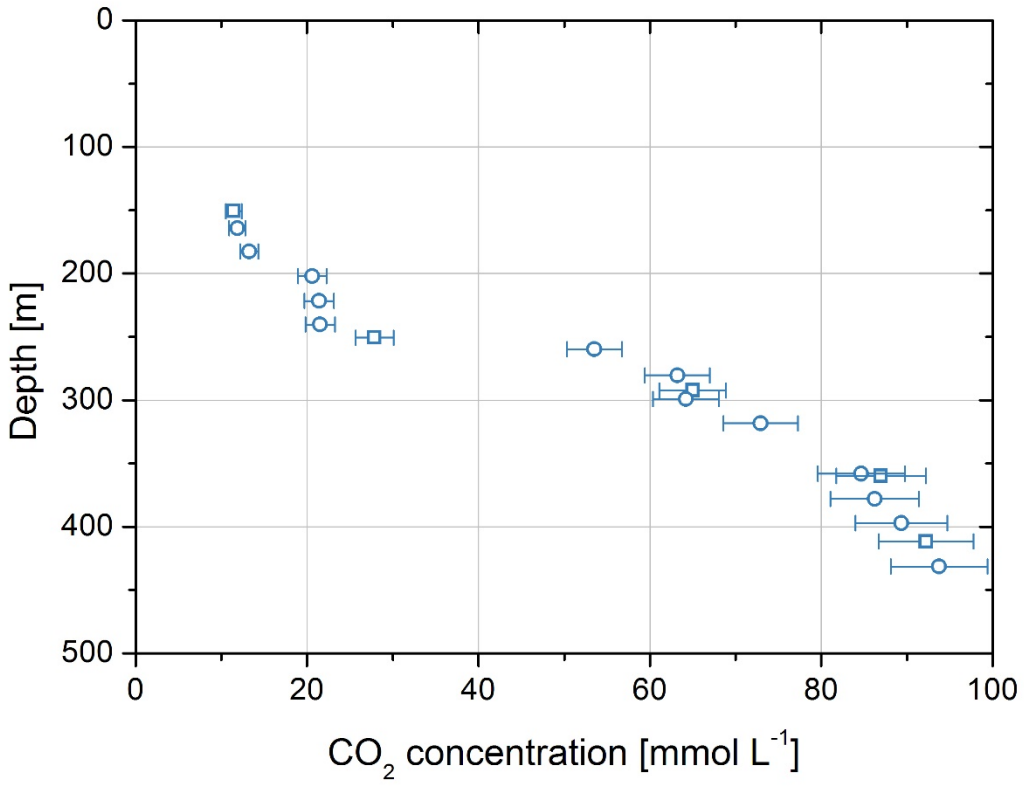

Figure 4.1: Carbon dioxide concentrations against depth in Lake Kivu measured by UFZ from samples taken with in-situ sampling bags. Samples were acquired in May/June 2017 (squares) and March 2018 (circles). Most of the samples were taken at Site 1, only the deepest measurement originates from sampling at Site 2.

4.2. Sampling with tubes combined with on-site mass spectrometry

The CO_2 concentrations measured by Eawag using the method described in section 2.6 are presented in Table 4.2 and Figure 4.2. Measurements in the depth range between 90 and 130 m were discarded, because at these depths, the water was already outgassing when brought to the surface, but the amounts of exsolved gas were too small to measure the gas flow.

Table 4.2: CO_2 concentrations measured by Eawag in Lake Kivu on 9-18 March 2018 using sampling tubes combined with on-site mass spectrometry.

Depth (m)	CO_2 concentration (mmol L^{-1})	Uncertainty of CO_2 concentration (mmol L^{-1})
11.2	0.033	0.0015
31.7	0.048	0.0021
50.4	0.048	0.0021
71.3	1.54	0.067
151.7	12.86	0.81
171.8	13.07	0.85
191.7	18.50	1.22
212.1	20.64	1.48
241.7	22.34	1.33
254.4	30.48	1.77
269.6	60.13	5.15
289.2	66.37	4.44
308.7	73.86	4.83
335.2	84.05	4.30
354.9	84.79	4.33
374.7	80.94	4.43
394.3	83.72	4.41
414.2	87.78	4.31
453.0	88.82	4.36

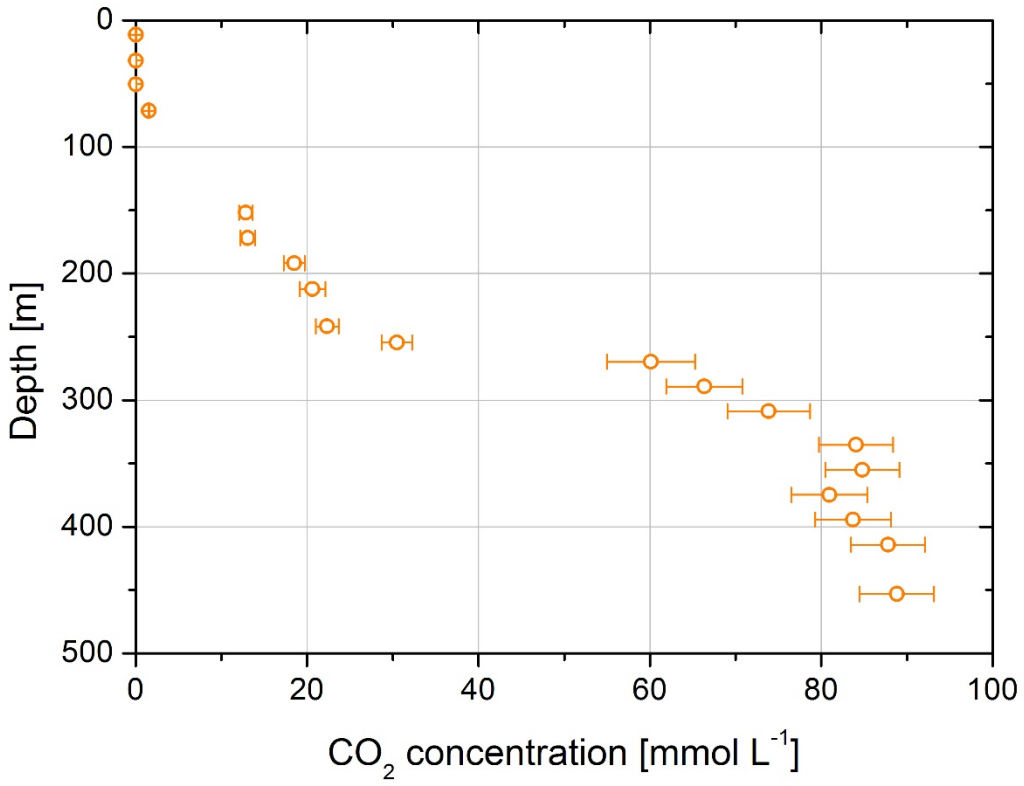

Figure 4.2: Carbon dioxide concentrations measured by Eawag in Lake Kivu on 9-18 March 2018 using sampling tubes combined with on-site mass spectrometry.

4.3. Comparison of carbon dioxide concentrations with different methods

Figure 4.3 shows a comparison of the two datasets of CO_2 concentrations measured in this inter-calibration campaign. Similar to the CH_4, there is good agreement between the datasets of UFZ and Eawag. Figure 4.4 shows the estimated smoothed CO_2 concentrations as a function of depth compared to the observations by UFZ and by Eawag. These were calculated in the same way as the smoothed CH_4 concentrations in section 3.5. The smoothed lines divert in the lowest water layers where the Eawag data is on average 7.4 % lower than the UFZ data below 400 m depth.

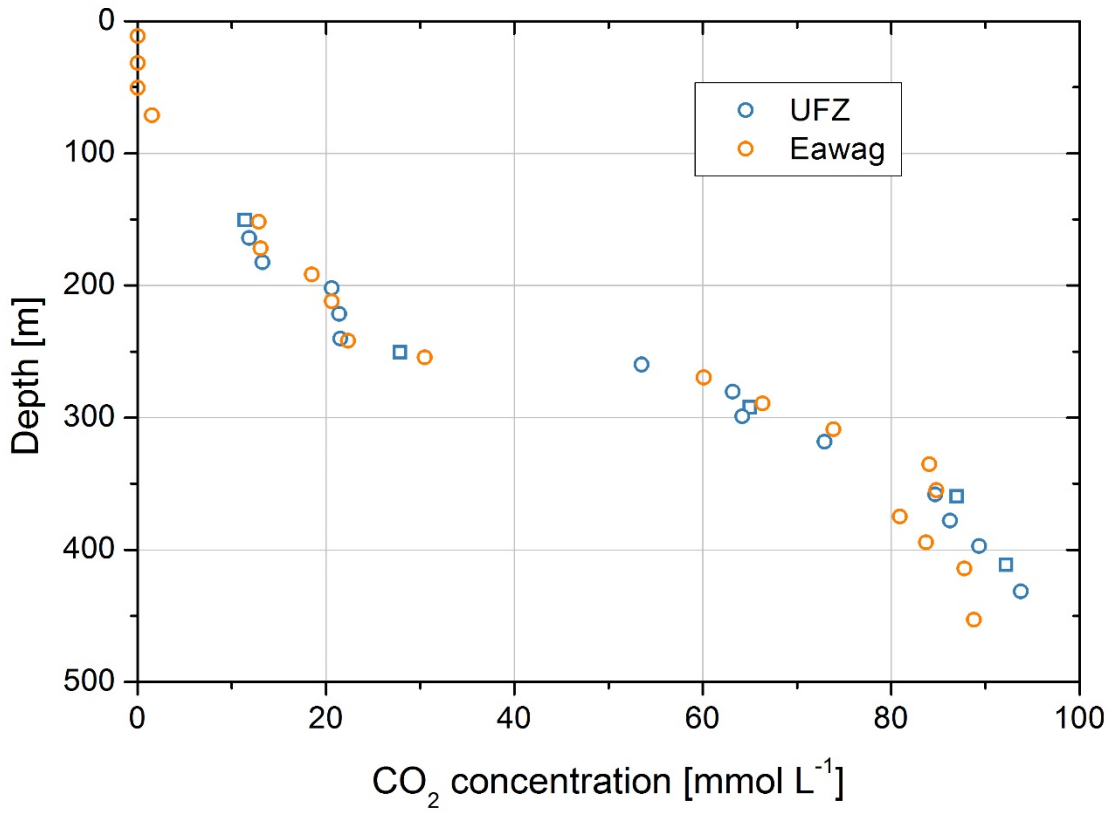

Figure 4.3: Summary of CO_2 concentrations measured in the intercalibration campaign.

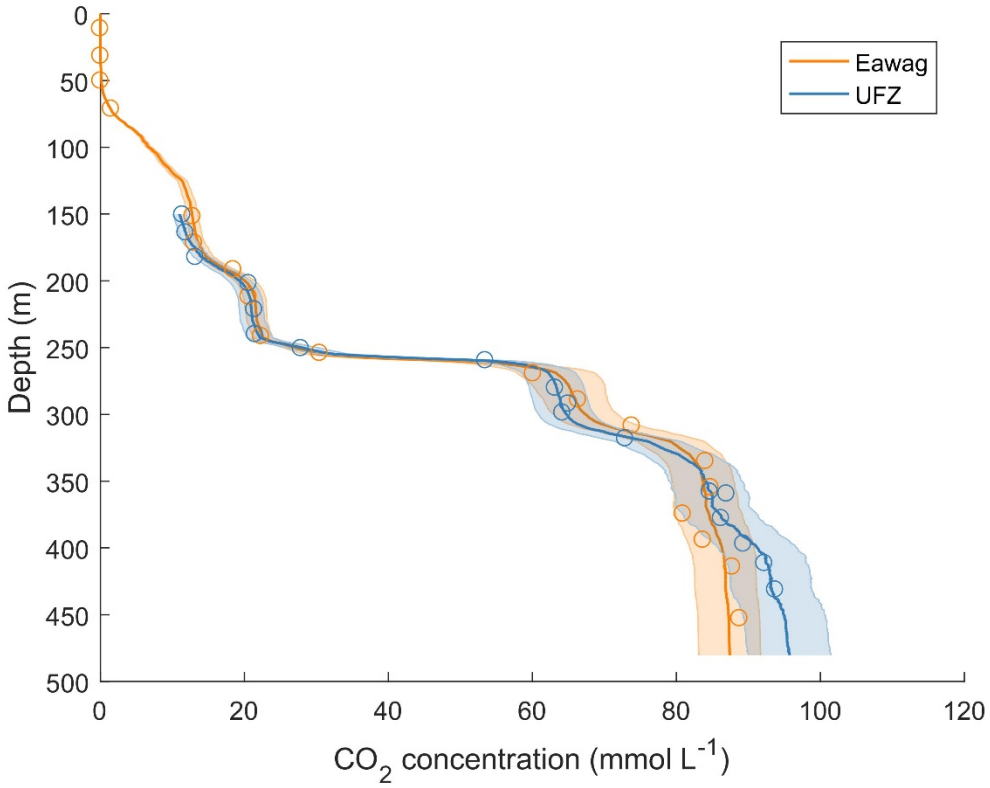

Figure 4.4: Smoothed CO_2 concentrations compared to concentrations measured by UFZ and Eawag. The shaded areas indicate approximate error ranges (interpolated relative errors between data points) around the smoothed lines.

5. Analytical results – Total gas pressure

5.1. In-situ gas pressure

The measurements with the two sensors agree very well with each other. Total dissolved gas pressures increase with depth, reaching close to 18 bars at the deepest measured location (Figure 5.1). A maximum gas saturation of ~50 %, calculated by dividing the measured total gas pressure by the sum of the hydrostatic pressure and the atmospheric pressure, is reached at 320 m depth.

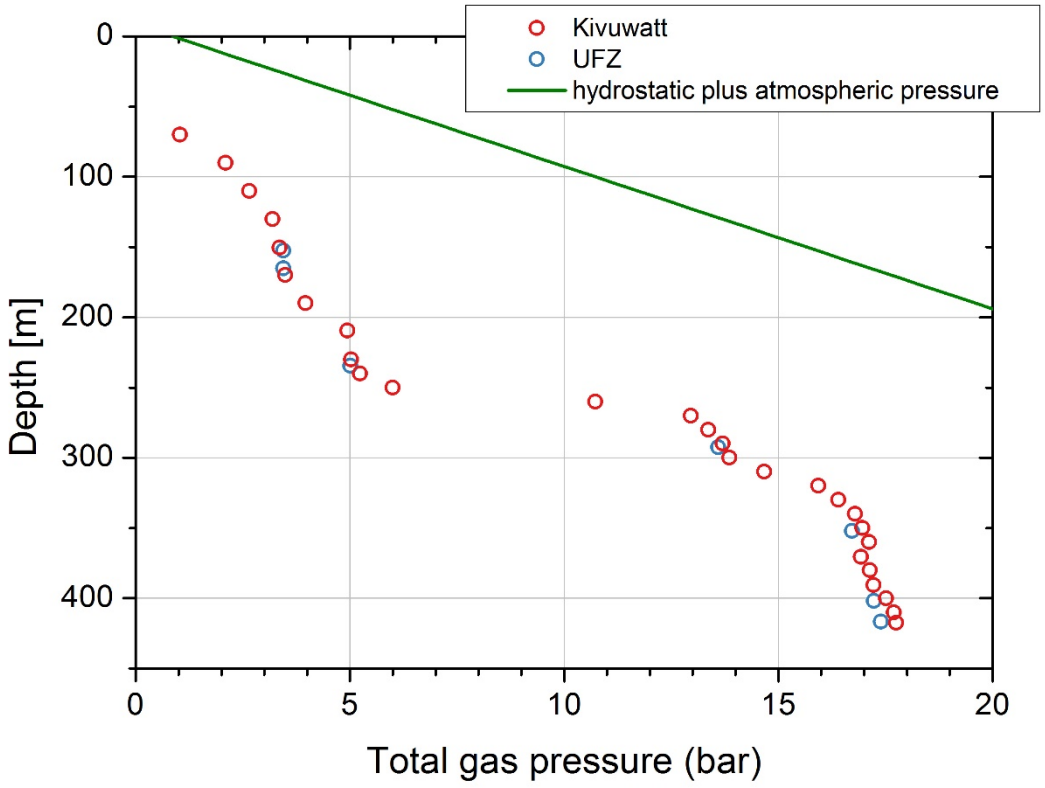

Figure 5.1: Total gas pressure measured by Kivuwatt with the Contros (May 2018) and by UFZ with the Pro-Oceanus (13th March 2018) gas pressure sensors against depth in Lake Kivu. The sum of the hydrostatic and atmospheric pressure (i.e., the in-situ pressure at a given depth) is shown for comparison.

For the concentration datasets of UFZ and Eawag, the total gas pressure can also be estimated by converting the smoothed concentration profiles of CH_4 (Figure 3.6) and CO_2 (Figure 4.4) to partial pressures with the inverse of the method described in section 2.7. Since the calculation of the fugacity coefficients requires knowledge of the fractions of CH_4 and CO_2 in the gas phase, this calculation must be done iteratively. The only gas that could additionally contribute measurably to the total gas pressure is atmospheric nitrogen N_2. In equilibrium with the atmospheric pressure at 860 mbar and its atmospheric

mixing ratio of 78 %, it would account for a partial pressure of 0.67 bar. Measurements of atmospheric noble gases indicate that their concentrations decline with depth to about half of the equilibrium with the atmosphere (Bärenbold et al., pers. comm.). If this is the case also for N_2, it would account for only 0.33 bar in the deep waters. The contribution of other dissolved gases such as noble gases or hydrogen sulfide (H_2S) to the total gas pressure is negligible. In this comparison we assumed a constant 0.67 bar contribution for N_2.

From the measurements of KivuWatt, only the partial pressure of CH_4 is available. The total gas pressure can therefore be estimated by adding the average partial pressure profile of CO_2 from the datasets of UFZ and Eawag, plus the same amount of N_2 as for the other datasets. The calculated total gas pressures are compared to the observed gas pressures in Figure 5.2.

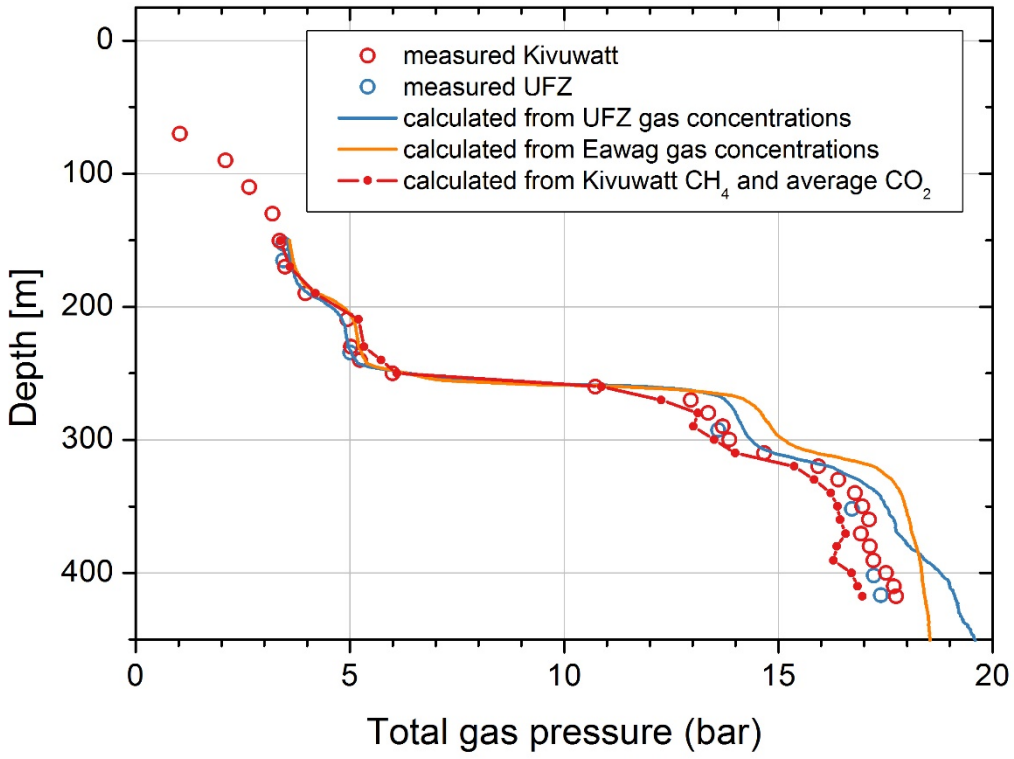

Figure 5.2: Total gas pressures calculated from the smoothed observed concentrations of methane and carbon dioxide by UFZ and Eawag plus 0.67 bar of N_2 (assumed to be in equilibrium with the atmosphere at any depth), and total gas pressure calculated from the observed CH_4 partial pressure of KivuWatt, the average smoothed concentrations of CO_2 from Eawag and UFZ datasets plus 0.67 bar of N_2.The three estimations are compared to the two direct total gas pressure measurements from in-situ sensors (circles).

The calculated gas pressures agree well with the observed gas pressures above the main gradient. Below the main gradient, between 270 and 420 m depth, the total gas pressures from UFZ and Eawag exceed the observed gas pressures on average by about 0.78 bar and 1.08 bar, respectively. These differences are reduced to 0.44 and 0.74 bar if N_2 is assumed to decrease with depth similar to the noble gases. This difference can be explained by an overestimation of CH_4, CO_2 or both gas concentrations, by an under-estimation of the total gas pressure, or by a combination of these three possibilities. However, similar to the discussion of the CH_4 concentrations of KivuWatt in section 3.5, part of this difference could also be caused by the conversion from concentrations to partial pressures, which adds some uncertainty. If the ratio of partial gas pressures to dissolved concentrations were somewhat smaller than resulting from the method described in section 2.7, this would decrease the gas pressures calculated from the concentrations of UFZ and Eawag, and increase the CH_4 concentrations calculated from the partial pressures by KivuWatt. In both cases, this would improve the agreement between the different datasets.

The total gas pressure calculated from the partial pressure of CH_4 measured by KivuWatt, the average partial pressure of CO_2 from UFZ and Eawag, and an assumed constant pressure of N_2 of 0.67 bar, is on average 0.63 bar below the total gas pressure measured with the same instrument. This difference increases to 0.97 bar if a partial pressure of only 0.33 is assumed for N_2. Since there is no conversion from concentrations to pressure in this case, this difference can only be explained if either the partial pressure of CH_4 is underestimated, the total gas pressure is overestimated, the CO_2 gas pressure is significantly higher than calculated from the observed concentrations, or by a combination of these three possibilities.

6. Discussion

6.1. Comparison with results from former campaigns

The smoothed average concentrations of CH_4 (section 3.5) and CO_2 (section 4.3) are compared to previous observations by Schmitz and Kufferath from 1952/4, K. Tietze from 1974/5, by M. Halbwachs and J.-C. Tochon from 2003 (published in Schmid et al., 2005), and by Schmid et al. (2005) in Figure 6.1 and Figure 6.2, respectively.

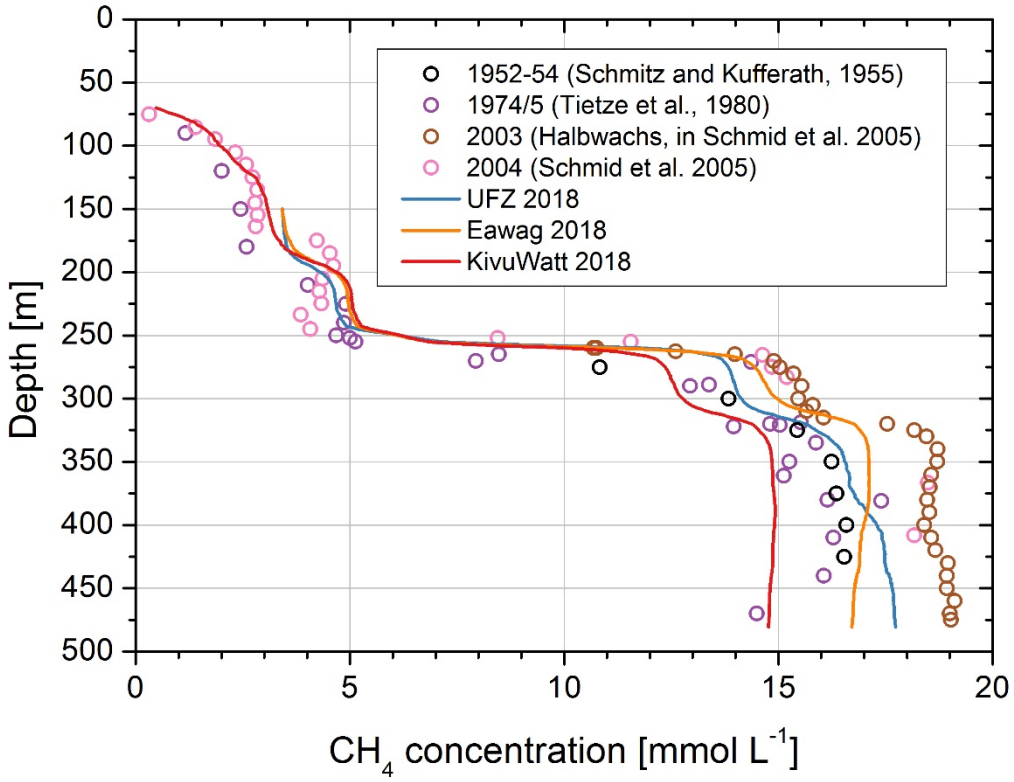

Figure 6.1: Smoothed methane concentration from this study compared to selected previously published observations.

The figures show relevant differences between the datasets. For the management of the lake, both considering commercial CH_4 extraction and the risk of a gas outburst, the most important depth range is the resource zone below the main gradient. In this range, the concentrations measured by UFZ and Eawag during this campaign are approximately in the middle between those measured by K. Tietze in 1974/5 and those measured by M. Halbwachs and J.-C. Tochon in 2003. The measurements of KivuWatt are a few percent below the mean concentrations measured by Tietze.

For CO_2, the concentrations measured with the different methods agree better with each other. This is true for both the historical measurements and the measurements made during this campaign.

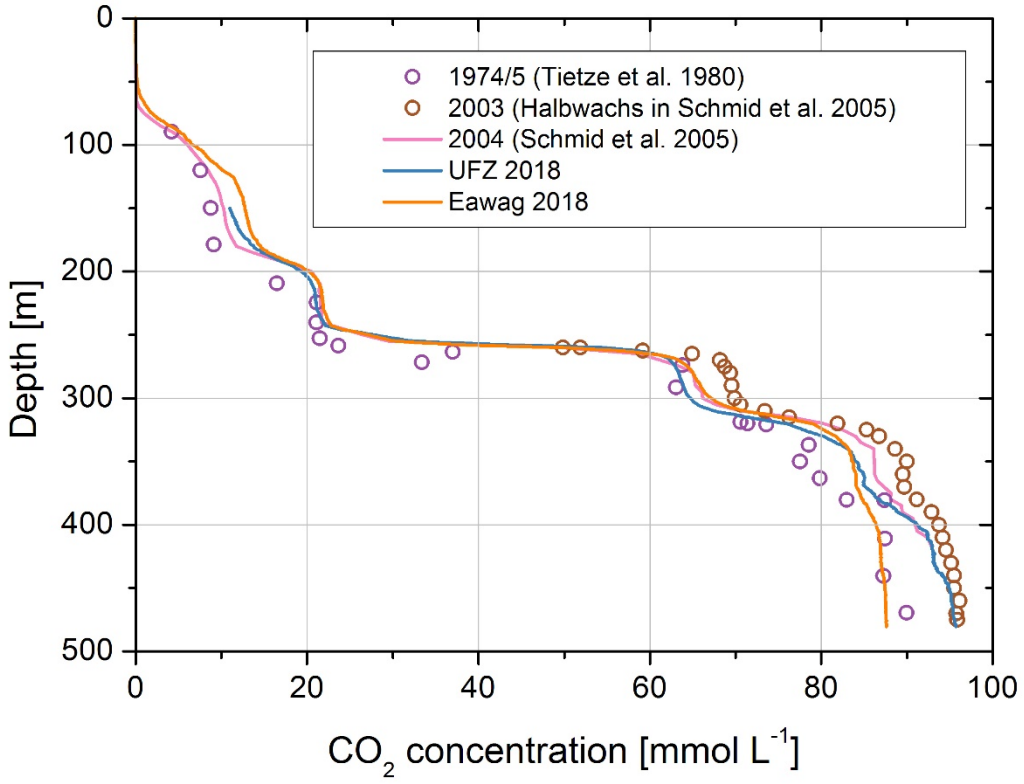

Figure 6.2: Smoothed CO_2 concentration from this study compared to selected previously published observations.

The larger discrepancies between the different datasets for CH_4 than for CO_2 indicate that the differences in the CH_4 concentrations are more likely caused by errors in the determination of the CH_4 content in the gas phase rather than errors in the determination of the total gas volume dissolved at a certain depth. In all methods except the direct determination of the partial pressure with in-situ sensors, the concentrations of CH_4 and CO_2 in the exsolved gases are measured using different types of instruments. Since the exsolved gases typically contain about 70 to 80 % of CO_2 and 20 to 30 % of CH_4, the same percentage error in the determination of the gas composition would result in approximately three times larger errors in the estimate of the CH_4 concentration than for the CO_2. Conversely, the same percentage error in the determination of the total gas content should result in only slightly larger errors for CH_4 than for CO_2 (depending on what fraction of the total CO_2 is exsolved in the different methods).

6.2. Assessment of the analytical methods

Table 6.1: Overview of advantages and disadvantages of the different methods used in the present intercalibration campaign for measuring concentrations of dissolved gases in Lake Kivu.

Method	**Advantages**	**Disadvantages**
In-situ partial gas pressures using Contros HydroC nondispersive infrared spectrometry	- Direct application in the field - Good reproducibility and stability - Provides also total gas pressure	- Long relaxation time (40 min) - Complicated calibration procedure - For estimating concentrations: additional uncertainty from converting partial pressures to concentrations
In-situ CH_4 concentrations using a Sub-Ocean prototype sensor	- Direct application in the field - Fast measurements - Yields almost continuous profiles	- Instrument not yet adapted to the high concentrations in Lake Kivu - Requires additional measurement of total gas pressure - Complicated calibration procedure - For estimating concentrations: additional uncertainty from converting partial pressures to concentrations
In-situ sampling in gas bags combined with gas chromatography	- Based on standard analytical methods - Reliable method with little calibration effort - Gas concentrations measured in the laboratory with instrument already available at LKMP	- High contribution of gas volume measurement to total uncertainty (could be improved) - For estimating gas pressures: additional uncertainty from converting concentrations to gas pressures
Sampling with tubes combined with on-site mass spectrometry	- Concentrations in water and gas phase determined simultaneously with the same instrument - Concentrations of other gases (e.g. noble gases) can be determined at the same time	- High contribution of gas volume measurement to total uncertainty (could be improved) - Measurement with in-situ gas spectrometer is not straightforward, needs experience with the instrument. - Regular calibration of the instrument needed - Only a few depths can be sampled per day

6.3. Estimation of the methane storage

For estimating the CH_4 storage, the smoothed concentrations at 0.5 m intervals from section 3.5 were converted to L STP / L water (STP: standard temperature and pressure of 1 atm and 0°C) with a molar gas volume of 22.414 L/mol. Concentrations were then multiplied by the lake area at the same depth determined by K.A. Ross from the blended bathymethric data of Ross et al. (2013) and the bathymetry of Lahmeyer and Osae (1998), and integrated over different depth ranges to provide the gas volumes given in Table 6.2. These values can be compared to the CH_4 contents estimated for the resource zone (44.7 km^3) and the potential resource zone from 200 to 260 m depth (8.5 km^3) by Wüest et al. (2012) based on the concentrations measured by M. Halbwachs and J.-C. Tochon in 2003.

Table 6.2: Total content of methane (km^3 STP) in different depth ranges of Lake Kivu estimated from the datasets collected in this study. The resource zones are defined as in EWGL (2009), but including half of the bordering gradients.

Depth range (m)	Eawag	UFZ	Kivuwatt	CNRS	average	median
0 to 70	-	-	-	0.1	0.1	0.1
70 to 150	-	-	6.6	6.5	6.5	6.5
150 to 200	5.8	5.8	5.6	-	5.8	5.8
200 to 260	8.5	8.2	8.6	-	8.4	8.5
260 to 300	12.5	12.1	10.8	-	11.8	12.1
300 to 350	14.7	13.8	12.5	-	13.7	13.8
350 to 400	9.5	9.4	8.3	-	9.1	9.4
400 to 480	5.5	5.7	4.8	-	5.3	5.5
Resource Zone (260 - 480 m)	42.2	40.9	36.4	-	39.8	40.9
Upper Resource Zone (260 - 310 m)	15.6	15.0	13.4		14.6	15.0
Lower Resource Zone (310 - 480 m)	26.6	25.9	23.1		25.2	25.9
Entire lake					60.6	61.5

6.4. Estimation of the recharge rate of methane

The new measurements do not confirm an increasing trend of CH_4 concentrations in Lake Kivu as initially reported in Schmid et al. (2005). The average observed concentrations are higher than those measured by K. Tietze in 1974/5 and lower than those measured by M. Halbwachs and J.-C. Tochon in 2003 (Figure 6.1; Schmid et al., 2005). We are convinced that this does not reflect the true dynamics of CH_4 in the lake, as the residence time of water in the resource zone is estimated to nearly 1000 years (Schmid and Wüest, 2012). In addition, the lower concentrations in the present study compared to the data of M. Halbwachs and J.-C. Tochon cannot be explained by the gas extraction of the KivuWatt power plant. The amount of CH_4 removed from the resource zone by the power plant from the start of operations until March 2018 was < 0.2 km^3 (KivuWatt, pers. comm.). We consider that the observed variability between the different datasets must be related to the limited accuracy of the various measurements.

In summary, we cannot confirm a significant recharge of CH_4 concentrations in Lake Kivu in the past decades on the base of the current data. We exclude that the CH_4 production is consistently as high as the

rate of 120 g C m^{-2} yr^{-1} (expressed in grams carbon contained in CH_4 produced per year and per m^2 of sediment area) that had been proposed by Schmid et al. (2005) to explain the differences between the observations of K. Tietze and those of M. Halbwachs and J.-C. Tochon. This value would correspond to a production of 0.24 km^3 yr^{-1} for the resource zone and 0.05 km^3 yr^{-1} for the potential resource zone. In this case CH_4 concentrations should now be about 5 to 10 % above the observations by M. Halbwachs and J.-C. Tochon in 2003. Our observations also do not agree with the CH_4 production in the resource zone of 93 g C m^{-2} yr^{-1} (0.18 km^3 yr^{-1}) as proposed by Pasche et al. (2011), which would correspond to a growth in concentrations by approximately 0.3 % per year.

A certain amount of CH_4 is continuously lost from the lake by upward transport and subsequent oxidation in the surface layer or (to a small extent) emission to the atmosphere (Pasche et al., 2011; Borges et al., 2011). To maintain the observed concentrations in the lake (steady-state assumption), the same amount of CH_4 needs to be produced in the lake. Schmid et al. (2005) estimated this steady-state production to be around 32 g C m^{-2} yr^{-1} (0.06 km^3 yr^{-1} in the resource zone and 0.013 km^3 yr^{-1} in the potential resource zone) to reach steady-state close to the observations of Tietze (1985), and Pasche et al. (2011) estimated it slightly higher at about 35 g C m^{-2} yr^{-1}.

6.5. Estimation of the CO_2 content in the lake

The CO_2 content of the lake was estimated with the same method as the CH_4 content in section 6.3, but only based on the smoothed concentrations calculated from the measurements of UFZ and Eawag (Figure 4.3). Larger uncertainties are located in the upper part (0 - 150 m) where the average value is based on a limited number of measurements, and for deep waters where the two datasets diverge. The volumes agree well within the uncertainties of the measurements with those estimated by Wüest and Schmid (2012) of 214 km^3 for the resource zone and 38 km^3 for the potential resource zone (200 to 260 m).

Table 6.3: Total content of CO_2 (km^3 STP) in different depth ranges of Lake Kivu estimated from the datasets collected in this study.

Depth range (m)	Eawag	UFZ	average
0 to 150	24.7	-	24.7
150 to 200	23.6	21.9	22.8
200 to 260	37.0	37.0	37.0
260 to 300	56.2	55.2	55.7
300 to 350	68.7	66.8	67.7
350 to 400	47.2	48.2	47.7
400 to 480	28.1	30.1	29.1
Resource zone (260 to 480 m)	200.2	200.3	200.2
Upper Resource Zone (260 to 310 m)	69.9	68.2	69.1
Lower Resource Zone (310 to 480 m)	130.3	132.1	131.2
Entire lake	285.6		284.8

7. Recommendations for monitoring gas concentrations

7.1. General considerations

Regular monitoring of the gas concentrations in the lake is important for three main purposes: (i) monitoring the concentrations as a base for assessing the risk of a gas outburst from the lake, (ii) estimating the concentrations as a base for the management of the gas extraction facilities, and (iii) monitoring the concentrations changes induced by the gas extraction facilities for assessing the impacts of these facilities. The requirements of the monitoring for these three different purposes and possible solutions are discussed in the following sections.

It is clear that such important measurements require regular survey of the instrument calibration. It should therefore be considered, in addition to the regular monitoring, to perform at regular intervals measurements with other instruments and/or involving other research teams to **ensure and document the quality of the measurements** and to detect possible instrument drift.

The following recommendations are based on the experiences made during this intercalibration campaign and the previous experience and knowledge of the involved experts. However, they should not replace a thorough analysis of different options for the monitoring that involves also other aspects such as available human and financial resources, maintenance of the laboratory facilities, and possible risks and opportunities. Also, monitoring of the activities of the gas extraction facilities and of possible ecological effects of gas extraction is not discussed in this report.

7.2. Monitoring gas concentrations for safety assessment

In principle, there are **three main scenarios** that can lead to an outburst of gases from Lake Kivu:

Scenario 1 is a **slow continuous increase of the gas concentrations** in the lake, which are thus approaching saturation and increase the risk that a sudden trigger (such as in the following scenarios) can trigger a gas eruption from the lake. Based on the comparison of the new measurements with previous observations (Figure 6.1 and Figure 6.2), there is no reason to assume that gas concentrations in the lake are changing by more than a few percent per decade under natural conditions. Since the total dissolved gas pressure is currently far below saturation, a significant increase in risk of a gas outburst can only occur on time scales of decades or even centuries. Local high saturation could also be artificially created at a specific depth by a gas extraction facility if gas-rich water (washing water or re-injection water) is injected at a depth where it is oversaturated. The latter scenario is covered in section 7.4.

Since the risk of a gas outburst is related to the total gas pressure and the partial pressures of the individual gases rather than their concentrations, an ideal monitoring system should directly observe the total gas pressure as well as the partial pressures of CH_4 and CO_2. This avoids additional uncertainty from the conversion of gas concentrations to gas pressures. Due to the slow time scales of changes, it should be sufficient to measure the gas pressures once every decade (but more frequent measurements could be

recommended to maintain the required capacity within the monitoring team). Since the expected temporal changes are still small over decades, the monitoring method should have a very high temporal stability. The comparison of the total gas pressure data between the Pro-Oceanus and the Contros sensors in the present study (Figure 5.1) seems to indicate that total gas pressure can be measured with high accuracy, even though this still needs further confirmation. To avoid reliance on a single sensor, and given that there is no need for more regular measurements, it could be recommended to use at least two different sensors for measuring total dissolved gas pressure. For the measurement of the partial pressures of the individual gases, we can currently not state with sufficient certainty that the quality of the available calibration procedures is adequate to ensure a sufficiently high accuracy for detecting changes in gas partial pressures on the time scales of the decades. We therefore recommend to further elaborate on the calibration of in-situ sensors for measuring partial pressures of CH_4 and CO_2.

Scenario 2 is a **change in the stratification** that could modify the gas saturation in different depth ranges. This could, for example, occur due to warming of the deep water by increased hydrothermal discharge, or by cooling of the surface waters due to unusual meteorological conditions (e.g., due to a very large volcanic eruption that would cool down global climate for several years). A warming of the deep water would decrease the solubility of the dissolved gases in the lake, and could potentially create an instability of the thermal stratification, thus leading to vertical mixing from below. A cooling from the surface could initiate deep mixing from above, but due to the high density difference, mixing below the main chemocline is not possible even for extreme assumptions. In both cases, gases could be transported to depths where they are closer or even above saturation. These scenarios have never been investigated in detail, but since the density stratification in Lake Kivu is currently extremely stable, very large changes in temperature (i.e., heat content) would be required for both these cases to happen, which means that even under extreme assumptions they cannot occur on time scales that are shorter than several months or years.

For monitoring the risk of a gas outburst induced by changes in the lake stratification, it seems appropriate to directly monitor the **changes in stratification** and **gas pressure** rather than changes in gas concentrations. Changes in stratification can be monitored by measuring vertical profiles of temperature and conductivity on a regular basis (e.g., **at monthly intervals**). These are standard methods, which can be performed with high accuracy and temporal stability. On the relatively short time scales of months or years relevant for this scenario, dissolved gases can be assumed to be affected mainly by the same transport processes as dissolved salts, and their distribution in the lake can therefore be estimated based on observed conductivities and established relationships between conductivity and gas concentrations. In case the monitoring of temperature and conductivity should indicate significant unexpected changes, further measurement campaigns would have to be designed depending on the observed signals to evaluate the possible causes for these changes. The measurements of total gas pressure from Pro-Oceanus and Contros sensors in the present study (Figure 5.1) indicate feasibility, high accuracy and good reproducibility. Although the conversion into gas concentration is difficult, it is the proper measure for assessing the risk imposed by gas pressure. In general, **one survey per year** should be sufficient, to follow changes.

Scenario 3 is an **extreme sudden event**, such as a volcanic eruption within the lake, which would create a rising plume of gas rich water, or a massive landslide creating a lake-internal tsunami that would move gas rich water to a depth where it is no longer saturated. The probabilities of occurrence of both these scenarios have only been insufficiently investigated until today. Schmid et al. (2004) estimated the size of a volcanic eruption within the lake that would be required to trigger a gas plume that could rise to a level where gas concentrations are above saturation, and concluded that an unusually large eruption would be required. However, that was only a preliminary analysis, which did not account for all processes that could occur in a multiphase flow.

Methods for assessing and monitoring the risk of such extreme events and the discussion of possible alarm systems for the population living around the lake in case such an extreme event should occur are outside the scope of the present report. However, given the large possible impact of a gas outburst, which could potentially kill the entire population living around the lake, it seems indicated to further discuss possible options for such monitoring and alarm systems, even if the probability for such an event to occur seems to be rather low. However, if volcanic activities are recorded, it may be indicated to perform measurements as outlined under scenario 2 at higher frequency as a first step.

7.3. Monitoring gas concentrations for the management of methane extraction facilities

Facilities for extracting CH_4 from Lake Kivu require accurate values of dissolved gas concentrations in the lake for the design and operation of their systems, especially at the depths from which they withdraw water, i.e., within the resource zone or the potential resource zone. For this purpose, the gas concentrations are a more relevant measure than the partial pressure of the gases, and therefore monitoring methods that directly measure gas concentrations are likely preferable to methods that measure partial pressures.

In summary, a measurement method for this purpose should:

- directly measure gas concentrations;
- have a high measurement accuracy with a maximal error of a few percent;
- have a good reproducibility and stability over time scales of decades;
- be relatively easy to apply, including the calibration procedure, because it is likely that different people will apply the method in the future.

From the methods applied in this study, the method used by UFZ, where water is sampled into bags in-situ, the mass of water and the volume of exsolved gases are determined, and the concentrations in the gas phase are determined with a gas spectrometer, seems to best comply with these criteria. However, the method still has potential for improvement. For example, the accuracy for determining the exsolved gas volume can likely be improved, and the concentrations of dissolved gases remaining in the water, currently assumed to be in equilibrium, could be measured in addition. It should also be noted that significant maintenance is required to ensure the quality of gas measurements with the gas

chromatograph over time scale of decades. The method by Eawag produced similar results with a similar scatter as those of UFZ, but it is more difficult to implement in the field. Another option might be to re-consider the method applied by M. Halbwachs and J.-C. Tochon in 2003, which showed a very high repeatability. Since the measurements do not have to be repeated at high frequency, it could also be an option to use at least two methods at the same time.

Since the expected natural changes in concentrations are smaller than the accuracy of the measurements on time scales of several years, there is no need to perform such measurements at high frequency. Under natural conditions, one survey per decade would be sufficient. Measurements at a higher frequency should be implemented as soon as more gas extraction facilities will be operational and the modifications they induce in the stratification and gas concentrations could potentially affect the quality of the gas resource in the lake. From the present perspective, a time interval of five years between measurements is recommended.

7.4. Monitoring the impacts of gas extraction facilities on gas concentrations in the lake

Gas extraction facilities affect the gas concentrations in the lake by removing gas-rich water from the resource zone or the potential resource zone, and by re-injecting degassed water and re-injecting washing water. It is expected, based on numerical simulations (Wüest et al, 2009, Schmid et al., 2018), that gas extraction facilities that follow the management prescriptions (EWGL, 2009) will reduce rather than increase the risk of a gas outburst from the lake. However, given that projections can always be wrong, that gas extraction facilities may not work exactly as foreseen, and considering the unpredictable dynamics of the active volcanic system in the region, it is indispensable to carefully monitor the impacts of the gas extraction facilities on the lake and to reassess and adapt the management prescriptions in case the monitoring should indicate relevant unexpected developments.

Ideally, monitoring the impacts of gas extraction facilities on gas concentrations in the lake involves (i) measuring the background gas concentrations in the lake at time scales within which relevant changes are to be expected, (ii) observing gas concentrations in the lake in the near-field of the re-injection points of degassed water and washing water and (iii) monitoring the composition of the re-injected degassed water and the washing water in order to know the quality of the water that enters the lake.

For observing the **effect on background concentrations** in the lake, the same requirements and recommendations apply as for monitoring the concentrations for the management of the gas extraction facilities in section 7.3. The only difference is that the frequency of monitoring needs to be adapted to the extent of CH_4 extraction that is taking place. The frequency of monitoring should be linked to the combined amount of water that is withdrawn by all facilities. A new profile could, for example, be required every time that a layer of approximately 5 m thickness has been withdrawn. For example, the KivuWatt Phase 2 is expected to extract ~22 $m^3\ s^{-1}$ of water for a production of ~100 MW (KivuWatt, pers. comm.). At 350 m depth, the lake has an area of ~650 km^2. A layer of 5 m thickness corresponds to 3.3 km^3 of water and would be extracted with a flow of 22 $m^3\ s^{-1}$ within 4 to 5 years. Accordingly, the present KivuWatt Phase 1

extraction regime will require 16 to 20 years to withdraw the water layer between 345 and 350 m depth. The depth range affected by the degassed return flows can be accurately determined from observed changes in conductivity and temperature in CTD profiles, while the depth range of the returned washing water can be accurately determined from the pH profile.

Observing the **gas concentrations in the near-field of the return flows** (both for the degassed and the washing water) would require the ability to measure these concentrations at high spatial and temporal resolution, since the properties of the discharge plumes vary strongly both in space and time. This is not possible with the currently available measurement devices, but may be possible in the future, for example, if optical sensors for measuring gas concentrations in-situ with fast response time will become available. As long as this is not the case, gas concentrations in the near-field of return flows can only be estimated if the concentrations of the gases in the discharged water is known and the discharge plume can be characterized by measurements of other properties that can be measured with high spatial and temporal resolution. The depth range affected by the degassed return flows can be accurately determined from observed changes in conductivity and temperature in CTD profiles, while the depth range of the returned washing water can be accurately determined from the pH profile.

In order to assess the contributions of individual gas facilities on observed changes in the gas concentrations in the lake, and to be able to project the long-term development of these concentrations using numerical models, it is indispensable to monitor the **gas concentrations in the discharge flows**. There is an inherent difficulty with monitoring the gas concentrations in the re-injected water. The water contains gas bubbles, at least in the upper part of the re-injection pipe. It is very challenging to take a representative sample from such a two-phase flow. For this reason, the water should probably be sampled from as deep as possible from the re-injection pipe, which is technically not easy. Since this was not tested in the present campaign, we cannot seriously assess the suitability of the different methods for measuring the gas concentrations in the discharge flow.

The **washing water** is used to purify the extracted CH_4 from other gases such as CO_2 and H_2S. Based on previous estimates, the reinjected washing water must be assumed to contain concentrations of H_2S that are acutely toxic for fish and other aquatic organisms (Schmid et al., 2018). It also contains large amounts of dissolved CO_2, which are expected to decrease the pH in the receiving water. The washing water is not expected to contain significant amounts of dissolved CH_4. The composition of the washing water should be regularly monitored to assess its potential impacts on biota, especially if it is discharged at a depth where it can potentially affect organisms requiring oxic conditions, as it is today authorized with the governing Management Prescriptions (EWGL 2009). The present discharge depth for the KivuWatt gas extraction facility is 60 m. As the methods used in the present study mainly aimed at measuring high concentrations of dissolved CH_4 and CO_2 in the water column of the lake, they cannot be directly applied for monitoring the gas contents of the washing water. In the washing water, it is mainly important to monitor concentrations of dissolved H_2S and CO_2, as well as the pH. H_2S and pH can likely be determined using accurate CTD probes additionally equipped with a H_2S sensor. For CO_2, the main difficulty might be to collect representative samples of the washing water.

7.5. Methane monitoring under the aspect of technical capabilities and skills

Independent from the recommendations in sections 7.2 to 7.4 for the methane monitoring at Lake Kivu based on the scientific knowledge, aspects of technical capabilities and skills also need to be considered.

For the monitoring of classical chemical parameters such as nutrients or trace element concentrations, standard measurement methods and procedures for quality assurance exist which are routinely performed by numerous laboratories worldwide. The extremely high gas concentrations in Lake Kivu are unique, and therefore, measurement methods have to be designed specifically for the purpose of monitoring the gas concentrations in this lake. This also means that the staff at the local laboratory of the Lake Kivu Monitoring Program, but also in general staff at laboratories elsewhere, do not have relevant experience with conducting these measurements.

The **risk of suboptimal sampling** and sample preparation, and consequently of producing analytical data with substandard quality is therefore higher for the gas monitoring at Lake Kivu than for standard lake monitoring programs. To reduce this risk and to increase the routine of the involved staff, it is therefore recommended to **perform monitoring activities more frequently** than required based only on the scientific recommendations.

Regular monitoring at a high frequency independent of the scientific needs has the following additional benefits:

- Development of routine skills and capabilities in sampling, calibration and determination of gas concentrations for the laboratories and staff involved;
- Possibility to test adaptations of measurement methods and to implement improvements;
- Easier and faster detection and mitigation of problems in the monitoring system (sampling procedure or analytical techniques), which will be observed as outliers in the dataset;
- Reduction of the uncertainty caused by random variations in the measurement methods, and consequently higher probability to detect small trends in concentrations;
- Increased confidence in the quality of the data and the competence of the monitoring team as a relevant base for discussing lake management strategies.

The assessment of the chemical status of surface waters in Germany according to the Water Framework Directive (WFD, European Commission, 2009) is based on a regular monitoring once-a-month for priority substances or once-per-three-months for other pollutants (Blonzik et al 2004). These monitoring frequencies according to WFD, Annex V 1.3.4, result in a certain confidence and precision. More frequent sampling may be necessary, e.g., to detect long-term changes, to estimate pollution loads, and to achieve acceptable levels of confidence and precision in assessing the status of water bodies.

Based on these facts, it is recommended to initially monitor gas concentrations in Lake Kivu at a regular interval of, e.g., two months for a test phase of five years. Subsequently, an assessment of the quality of the 5-year-dataset and the capacities of the monitoring team should be the base for recommending a long-term monitoring strategy.

7.6. Tasks beyond monitoring

It is clear that not all developments can be foreseen from the current knowledge. Some features may be understood better in some years from now, as science and technical evolution are progressing. An awareness must be guaranteed that any observed development must be predicted with its long-term effect to counteract undesirable consequences. Sometimes this can be done with simple projections. In more complex situations, more sophisticated approaches may be required, such as numerical models (e.g. Schmid et al., 2018).

Also, technical development should be followed, and new solutions should be tried out. For example, the above-mentioned submersible, optical sensors may become available for gas measurements. We encourage to stay up to date with these developments and also to become active in improving available technical solutions for the purposes of a sustainable management of Lake Kivu

Acknowledgements

The authors would like to thank the entire team of LKMP for their excellent support during the preparation and execution of the field work, and Nic Spycher (Berkeley Lab) and Zaman Ziabakhsh-Ganji (TU Delft) for providing information and code for the conversion between gas partial pressures and concentrations.

References

Blondzik K, Claussen U, Füll C, Heidemeier J, Herata H, Irmer U, Jekel H, Lepom P, Markard C, Mohaupt V, Naumann S, Rechenberg B, Rechenberg J, Richter S, Wolter R, Wunderlich D (2004). Die Wasserrahmenrichtlinie – Neues Fundament für den Gewässerschutz in Europa. Bonifatius, Parderborn, p. 105.

Boehrer B, Yusta I, Magin K, Sanchez-España J (2016). Quantifying, assessing and removing the extreme gas load from meromictic Guadiana pit lake, Southwest Spain. *Science of the Total Environment* 563-564: 486-477.

Borges AV, Abril G, Delille B, Descy J-P, Darchambeau F (2011). Diffusive methane emissions to the atmosphere from Lake Kivu. *Journal of Geophysical Research* 116: G03032, doi: 10.1029/2011JG001673.

Brennwald MS, Schmidt M, Oser J, Kipfer R (2016). A portable and autonomous mass spectrometric system for on-site environmental gas analysis. *Environmental Science & Technology* 50(24): 13455-13463.

Cai W-J, Wang Y (1998). The chemistry, fluxes, and sources of carbon dioxide in the estuarine waters of the Satilla and Altamaha Rivers, Georgia. *Limnology and Oceanography* 43(4): 657-668.

Damas H (1937). Quelques caractères écologiques de trois lacs équatoriaux: Kivu, Edouard, Ndalaga. *Annales de la Société Royale Zoologique de Belgique* 68: 121-135.

Degens ET, Deuser WG, von Herzen RP, Wong H-K, Wooding FB, Jannasch HW, Kanwisher JW (1971). Lake Kivu expedition: Geophysics, hydrography, sedimentology. Woods Hole Oceanographic Institution, Report 71-52.

Degens ET, von Herzen RP, Wong H-K, Deuser WG, Jannasch HW (1973). Lake Kivu: structure, chemistry and biology of an East African Rift Lake. *Geologische Rundschau* 62: 245-277.

Esper G, Lemming W, Beckermann W, Kohler F (1995). Acoustic determination of ideal gas heat capacity and second virial coefficient of small hydrocarbons. *Fluid Phase Equilibria* 105: 173-192.

European Commission (2009). Common Implementation strategy for the water framework directive (2000/60/EC), Technical Report - 2009 – 025, ISBN 978-92-79-11297-3, p. 15

EWGL (2009). Management prescriptions for the development of Lake Kivu gas resources, Ministry of Infrastructure of the Republic of Rwanda and the Ministry of Hydrocarbons of the Democratic Republic of the Congo.

Fietzek P, Fiedler B, Steinhoff T, Körtzinger A (2014). In situ Quality Assessment of a Novel Underwater pCO_2 Sensor Based on Membrane Equilibration and NDIR Spectrometry. *Journal of Atmospheric and Oceanic Technology* 31: 181-196.

Grilli R, Marrocco N, Desbois T, Guillerm C, Triest J, Kerstel E, Romanini D (2014). Invited Article : SUBGLACIOR: An optical analyzer embedded in an Antarctic ice probe for exploring the past climate. *Review of Scientific Instruments* 85: 1–8.

Grilli R, J. Triest J, Chappellaz J, Calzas M, Desbois T, Jansson P, Guillerm C, Ferré B, Lechevallier L, Ledoux V, Romanini D (2018). SUB-OCEAN: subsea dissolved methane measurements using an embedded laser spectrometer technology. *Environmental Science & Technol*ogy 52(18): 10543-10551.

Horn C, Metzler P, Ullrich K, Koschorreck M, Boehrer B (2017). Methane storage and ebullition in monimolimnetic waters of polluted mine pit lake Vollert-Sued, Germany, *Science of the Total Environment* 584-585: 1-10.

IOC, SCOR, IAPSO (2010). The international thermodynamic equation of seawater - 2010: Calculation and use of thermodynamic properties. Intergovernmental Oceanic Commission, Manuals and Guides 56, UNESCO, 196 pp.

Kusakabe M, Tanyileke GZ, McCord SA, Schladow SG (2000). Recent pH and CO_2 profiles at Lakes Nyos and Monoun, Cameroon: implications for the degassing strategy and its numerical simulation. *Journal of Volcanology and Geothermal Research* 97(1-4): 241-260.

Lahmeyer and Osae (1998). Bathymetric survey of Lake Kivu. Final report., Republic of Rwanda, Ministry of Public Work, Directory of Energy and Hydrocarbons, Kigali.

Murray CN, Riley JP (1971). The solubility of gases in distilled water and sea water—IV, carbon dioxide. *Deep-Sea Research* 18: 533–541.

Pasche N, Schmid M, Vazquez F, Schubert CJ, Wüest A, Kessler JD, Pack MA, Reeburgh WS, Bürgmann H (2011). Methane sources and sinks in Lake Kivu. *Journal of Geophysical Research - Biogeosciences* 116: G03006.

Rettich TR, Handa P, Battino R, Wilhelm E (1981). Solubility of gases in liquids. 13. High-precision determination of Henry's constants for methane and ethane in liquid water at 275 to 328 K. *Journal of Physical Chemistry* 85(22): 3230-3237.

Robb WL (1968). Thin silicon membranes. Their permeation properties and some applications. *Annals* of the *New York Academy* of *Sciences* 146: 119–137.

Robinson RA (1954). The vapour pressure and osmotic equivalence of sea water. *Journal of the Marine Biological* Association *of the* United Kingdom 33(2): 449-455.

Ross KA, Smets B, De Batist M, Hilbe M, Schmid M, Anselmetti FS (2014). Lake-level rise in the late Pleistocene and active subaquatic volcanism since the Holocene in Lake Kivu, East African Rift. *Geomorphology*, 221: 274-285.

Ross KA, Gashugi E, Gafasi A, Wüest A, Schmid M (2015). Characterisation of the subaquatic groundwater discharge that maintains the permanent stratification within Lake Kivu; East Africa. *PLoS One*, 10(3): e0121217.

Sander R (2015). Compilation of Henry 's law constants (version 4.0) for water as solvent. *Atmospheric Chemistry and Physics* 15: 4399–4981.

Schmid M, Tietze K, Halbwachs M, Lorke A, McGinnis D, Wüest A (2004). How hazardous is the gas accumulation in Lake Kivu? Arguments for a risk assessment in light of the Nyiragongo Volcano eruption of 2002. *Acta vulcanologica*, 14/15 (2002-2003): 115-121.

Schmid M, Gerber C, Bärenbold F, Wüest A (2018). Assessment of the effects of different scenarios for methane extraction from Lake Kivu based on numerical modelling, Eawag, Kastanienbaum.

Schmid M, Halbwachs M, Wehrli B, Wüest A (2005). Weak mixing in Lake Kivu: New insights indicate increasing risk of uncontrolled gas eruption. *Geochemistry Geophys. Geosystems* 6: Q07009

Schmid M, Wüest A (2012). Stratification, mixing and transport processes in Lake Kivu. In: Descy JP, Darchambeau F, Schmid M (Eds.), Lake Kivu: *Limnology and biogeochemistry of a unique tropical lake*. Aquatic Ecology Series. Springer, pp. 13-29.

Schmitz DM, Kufferath J (1955). Problèmes posés par la présence de gaz dissous dans les eaux profondes du lac Kivu. *Bulletin des Séances de l' Académie Royale des Sciences Coloniales*, 1: 326-356.

Tassi F, Vaselli O, Tedesco D, Montegrossi G, Darrah T, Cuoco E, Mapendano MY, Poreda R, Delgado Huertas A (2009). Water and gas chemistry at Lake Kivu (DRC): Geochemical evidence of vertical and horizontal heterogeneities in a multibasin structure. *Geochemistry Geophysics Geosystems*, 10, Q02005.

Tietze K (1978). Geophysikalische Untersuchung des Kivusees und seiner ungewöhnlichen Methangaslagerstätte - Schichtung, Dynamik und Gasgehalt des Seewassers. PhD Thesis Thesis, Christian-Albrechts-Universität Kiel, 150 pp.

Tietze K, Geyh M, Müller H, Schröder L (1980). The genesis of methane in Lake Kivu (Central Africa). *Geologische Rundschau* 69: 452-472.

Triest J, Chappellaz J, Grilli R (2017). Patent 08276-01: System for fast and in-situ sampling of dissolved gases in the ocean, CNRS, Grenoble, France.

Tuttle ML, Lockwood JP, Evans WC (1990). Natural hazards associated with Lake Kivu and adjoining areas of the Birunga volcanic field, Rwanda and Zaire, Central Africa. 90-691, USGS.

Weiss RF (1974). Carbon dioxide in water and seawater: the solubility of a non-ideal gas. *Marine Chemistry* 2: 203-215.

Wiesenburg DA, Guinasso NL (1979). Equilibrium solubilities of methane, carbon monoxide and hydrogen in water and seawater. *Journal of Chemical and Engineering Data* 24(4): 357-360.

Wilke CR (1950) A viscosity equation for gas mixtures. *The journal of chemical physics* 18: 517-519.

Wüest A, Jarc L, Schmid M (2009). Modelling the reinjection of deep-water after methane extraction in Lake Kivu, Belgian Technical Cooperation (BTC) and Ministry of Infrastructure of the Government of Rwanda (Mininfra).

Wüest A, Jarc L, Bürgmann H, Pasche N, Schmid M (2012). Methane formation and future extraction in Lake Kivu. In: Descy JP, Darchambeau F, Schmid M (Eds.), *Lake Kivu: Limnology and biogeochemistry of a unique tropical lake.* Aquatic Ecology Series. Springer, pp. 165-180.

Wüest A, Piepke G, Halfman JD (1996). Combined effects of dissolved solids and temperature on the density stratification of Lake Malawi. In: Johnson TC, Odada EO (Eds.), *The Limnology, Climatology and Paleoclimatology of the East African Lakes*, Gordon and Breach, pp. 183-202.

Yamamoto S (1976). Solubility of methane in distilled water and sea water. *Journal of Chemical and Engineering Data* 21(1): 78-80.

Ziabakhsh-Ganji Z, Kooi H (2012). An Equation of State for thermodynamic equilibrium of gas mixtures and brines to allow simulation of the effects of impurities in subsurface CO_2 storage. *International Journal of Greenhouse Gas Control* 11S: S21-S34.